

FAUNAL SUCCESSION AND GEOCHEMICAL ANALYSIS OF CARBONATE FACIES
CHANGES ALONG THE LATE PERMIAN MASS EXTINCTION BOUNDARY IN THE
NANPANJIANG BASIN, SOUTH CHINA: A POTENTIAL ARGUMENT FOR OCEAN
ACIDIFICATION AND ITS IMPLICATIONS

A Thesis

Presented to the Honors Program of

Angelo State University

In Partial Fulfillment of the

Requirements for Highest University Honors

BACHELOR OF SCIENCE

By

MAIGAN ANSLI DUNLAP

May 2017

Major: Geoscience

FAUNAL SUCCESSION AND GEOCHEMICAL ANALYSIS OF CARBONATE FACIES
CHANGES ALONG THE LATE PERMIAN MASS EXTINCTION BOUNDARY IN THE
NANPANJIANG BASIN, SOUTH CHINA: A POTENTIAL ARGUMENT FOR OCEAN
ACIDIFICATION AND ITS IMPLICATIONS

by

MAIGAN ANSLI DUNLAP

APPROVED:

Dr. Fawn Last, Chair
Assistant Professor of Geoscience

Dr. Heather Lehto
Assistant Professor of Geoscience

28 April 2017
Date Successfully Defended and
Approved by Advisory
Committee

APPROVED:

Dr. Shirley M. Eoff 12 May 2017
Director of the Honors Program

ACKNOWLEDGEMENTS

A massive thank you goes to my adviser Dr. Fawn Last for her incredible words of wisdom, never-ending support, and patience (especially when it came to my incessant emails). She serves as the absolute embodiment of what it means to be a scientist, mentor, and friend in the most genuine way possible. Thank you for restoring my passion for geology and reminding me to always follow my heart. Additionally, I have to thank Dr. Heather Lehto for serving as my additional committee member, and taking time out of her busy schedule to guide and help me throughout this process. Without my committee, this would not be possible. I am blessed to have such strong female examples in the geology program at Angelo State. I owe Dr. Shirley Eoff a huge thank you as well. No matter what I pursued at Angelo State University, she backed me one-hundred percent and I owe all of the wonderful things I have been able to do during my undergraduate career to her decision to invest her time and energy into me. Moreover, Dr. Daniel Lehrmann has been instrumental to this undergraduate thesis as he supplied microbialite samples which are the foundation of this project. Without him, this project would not be possible.

Thank you to Isotech Laboratories Incorporated for their swift turnaround of stable isotope results. Thank you to the Angelo State University Undergraduate Faculty Mentored Research Grant program for funding this project and also trips to present this research at conferences. Most importantly, I have to thank my friends and family for supporting me throughout this entire process and inspiring me to wholeheartedly devote myself to what I love. I am so lucky to have each and every one of you in my life and you all serve as examples of kindness, brilliance, and genuinity all wrapped into one.

ABSTRACT

The late Permian mass extinction is considered the largest extinction event in Earth's history with over 90% of marine and 70% of terrestrial species becoming extinct as a result (Lehrmann et al., 2015). The Nanpanjiang Basin in southern China contains multiple drowned carbonate platforms that are a record of the Permian-Triassic boundary. Data of two subsections from the Tianwan section of the Tian'e platform in the Nanpanjiang Basin consist of Permian carbonates, the altered truncation surface of the Permian-Triassic boundary as well as Triassic microbialites.

Analysis of 1) faunal succession, 2) faunal dominance, 3) stable isotopes and 4) diagenetic structures contributes to the understanding of the environmental conditions during the late Permian to early Triassic. Data collected shows a trend from skeletal packstone to microbial boundstone from the Permian to Triassic respectively. Stable isotope analysis of $\delta^{13}\text{C}$ and $\delta^{18}\text{O}$ data up section both show large excursions at the extinction boundary.

TABLE OF CONTENTS

ACKNOWLEDGEMENTS.....	iii
ABSTRACT.....	iv
TABLE OF CONTENTS.....	v
LIST OF FIGURES	vi
BACKGROUND	1
INTRODUCTION	6
METHODOLOGY	11
RESULTS	18
Faunal Succession: Tianwan subsection 1 and 2	18
Stable Isotope Geochemistry	26
Diagenetic Structures	30
DISCUSSION	33
Faunal Succession and Dominance.....	33
Stable Isotopes	36
Diagenetic Structures	39
FUTURE WORK.....	42
CONCLUSION AND IMPLICATIONS.....	46
LITERATURE CITED	52
BIOGRAPHY	58

LIST OF FIGURES

Figure 1. Paleogeographic map of Earth during the Permian-Triassic.....	1
Figure 2. Location of the Tian'e platform within the Nanpanjiang Basin	2
Figure 3. Outcrop photo of the Heshan Formation from the Tianwan section.....	3
Figure 4. Carbon dioxide values from the present to the Cambrian	7
Figure 5. Quadrat sampling method of point counting	12
Figure 6. Examples of fossils spanning the Permian –Triassic	13
Figure 7. Faunal succession of the first subsection of the Tianwan section.....	18
Figure 8. Simpson's Index vs. Simpson's Index of Diversity	19
Figure 9. Shannon's Index for the first subsection of the Tianwan section.....	21
Figure 10. Faunal succession of the second subsection of the Tianwan section.	22
Figure 11. Simpson's Index vs. Simpson's Index of Diversity	23
Figure 12. Shannon's Index for the first subsection of the Tianwan section.....	25
Figure 13. $\delta^{13}\text{C}$ values across the late Permian mass extinction: subsection 1	26
Figure 14. $\delta^{18}\text{O}$ values across the late Permian mass extinction: subsection 1	27
Figure 15. $\delta^{13}\text{C}$ values across the late Permian mass extinction: subsection 2	28
Figure 16. $\delta^{18}\text{O}$ values across the late Permian mass extinction: subsection 2	29
Figure 17. Diagenetic structures from both subsections	30
Figure 19. Proposed aragonite fan deposition model.....	40

BACKGROUND

During the late Permian Period, the Nanpanjiang Basin of south China was a deep marine embayment relatively close to the equator in the Laurasian supercontinent of Pangea. Moreover, the Nanpanjiang Basin was a constituent of the Tethys Ocean as were parts of Vietnam, Saudi Arabia, Turkey, Iran, Hungary, and Japan (Lehrmann et al., 2015). The Tethys Ocean was open to the Panthalassa Ocean allowing widespread circulation and equilibration during the Permian and into the Triassic (Figure 1) (Kershaw et al., 2012).

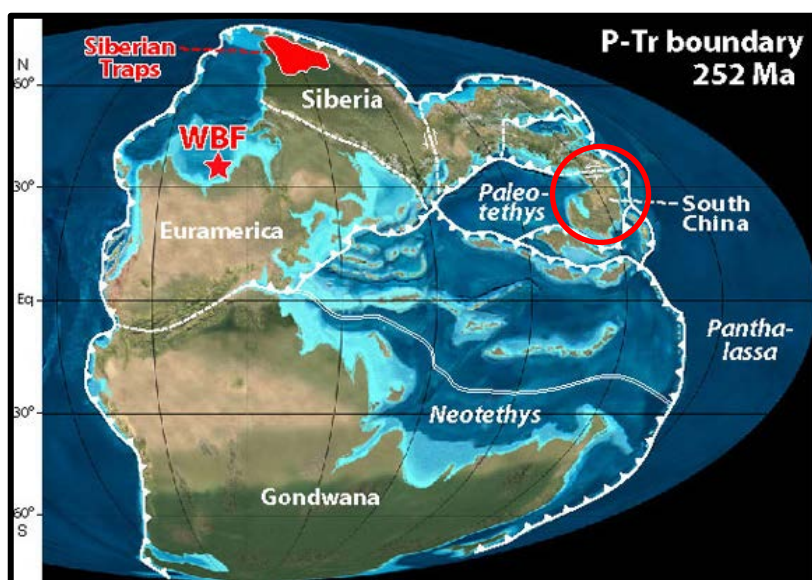


Figure 1. Paleogeographic map of Earth during the Permian-Triassic. The map shows the proximity of the Siberian Traps Igneous Province and location of South China circled in red along the paleo Tethys (<http://www.spaceref.com/news/viewpr.html?pid=35965>).

The Nanpanjiang Basin was bordered to the north by the Yangtze Platform which served as a source of sediments that fed into the basin and provided a rich nutrient load (Figure 2) (Lehrmann et al., 2015). The Nanpanjiang Basin was a constituent of the Yangtze block microcontinent and was accreted to northern China during the Triassic allowing for

drowning of the carbonate platforms due to sea level rise (Lehrmann et al., 1998). Facies description of the Nanpanjiang Basin consist of open marine, subtidal Permian units as a result of the widening of the basin and early Triassic units are made up of microbial boundstones indicative of an open marine, aerobic subtidal depositional environment as a result of sea level rise (Lehrmann et al., 1998). Of particular interest to this research is the basin's close proximity to the Siberian Traps Igneous Province at the time of emplacement (Figure 1).

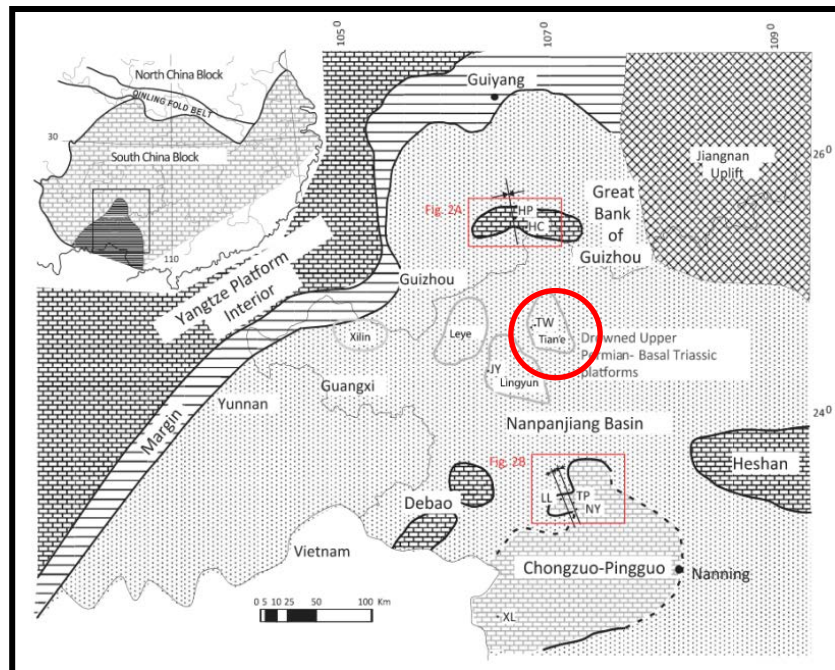


Figure 2. Location of the Tian'e platform within the Nanpanjiang Basin circled in red. Additional drowned carbonate platforms are included in the figure, but the Tian'e platform is the platform pertinent to this research (with permission from Lehrmann et al., 2015).

Within the Nanpanjiang Basin are multiple solitary, carbonate platforms, one of which being the Tian'e platform which contains two subsections of the Tianwan section. The Tianwan section is a drowned, carbonate platform that spans the before, during, and after periods of

the late Permian mass extinction event and serves as a key locality to understanding the mechanisms of Earth's greatest mass extinction (Figure 2) (Lehrmann et al., 2015).

The Tianwan section of the Tian'e platform is made up of the Heshan and Bana Formation which are described by Lehrmann (personal communication) as the:

- Heshan Formation- cherty, skeletal packstone with fossils constituting the grains and overlain by four meters of microbial boundstone marked by nodular bedding. Stylolites and aragonite fans are found throughout (Figure 3).
- Bana Formation- sand rich beds 1.5 centimeters thick interbedded with black shales indicative of transgressive or sea level rise sequence. There are no fossils present. Stylolites and aragonite fans are found throughout.



Figure 3. Outcrop photo of the Heshan Formation from the Tianwan section. Bana Formation not pictured. Also pictured is the nodular bedding in the microbial boundstone (circled in red) (Lehrmann, personal communication).

The genesis of the microbialites overlying the packstone in both subsections of the Tianwan section is debated. Hypotheses for the formation of this sequence range from reduced grazing and competition to changes in oceanic conditions/chemistries and even elevated calcium carbonate saturation in the oceans as a result of increased nutrient loading and ocean acidification (Lehrmann et al., 2015). Ocean acidification caused by dissolved CO₂ mixing with oceanic water to form carbonic acid during the late Permian is believed to have reduced the pH of the oceans and had a negative effect on carbonate sinks through the resulting dissolution (Hönisch et al., 2012). This is a fairly new hypothesis, but is intimately tied to observations in the Tianwan section including a dissolution/truncation surface with small caverns, isopachous cements, aragonite fans, and thick (>4 meters) microbialite facies post extinction (Lehrmann et al., 2015; Payne et al., 2007; Greene et al., 2012).

Work in this section continues but the microbialite facies and truncation surface have been outlined and discussed in Lehrmann et al. (2015). A summary of micro and macroscopic features of Tianwan microbialites include nodular biostromes, thrombolytic structures, aragonite fans at the base of the microbialites, calcified coccoid cyanobacteria, cavities filled with micrite, packstone and wackestone, and pendant cements (Lehrmann et al., 2015). Furthermore, micro and macroscopic features of the truncation surface include a sharp and irregular surface with caverns below having lateral widths ranging from a few to 30 centimeters, a micritized zone within the Permian packstone, isopachous cement, and pendant cement (Lehrmann et al., 2015). The truncation surface is believed to be a direct result of increased $p\text{CO}_2$, SO₂, and HCL from the Siberian Traps and has the potential to serve as an indicator of past ocean acidification. The goal of this research is to add both qualitative and quantitative data as further evidence of ocean acidification during the late

Permian mass extinction in the Tianwan section of the Tian'e platform. To formulate a general understanding of the Tianwan section, it is important to note that two subsections were sampled from within the Tianwan section. Both subsections are located along and sampled from a road-cut outcrop that exposes the Permian-Triassic boundary in the Tianwan section of the Nanpanjiang Basin. The subsections are laterally continuous with respect to their coinciding units (skeletal packstone and microbial boundstone) and are simply separate localities in the Tianwan section.

INTRODUCTION

Heralded as the “Great Dying”, the late Permian mass extinction is considered the largest mass extinction event of the “Big Five” to affect Earth’s biosphere (Erwin, 1994). It is estimated that 90% of marine and 70% of terrestrial species went extinct during the 60 ± 48 kyr extinction interval which, in terms of geologic time, is a blip in Earth’s history (Bond and Grasby, 2016). The duality of the rapidity and magnitude of the late Permian mass extinction is both alarming and incredibly interesting, making its origins a heavily debated topic in the realm of paleontology and paleoclimatology.

Hypotheses for the cause of late Permian mass extinction stems from the emplacement of the Siberian Traps Igneous Province. The eruption of the Siberian Traps was a million year period during the late Permian of enormous flood basalt deposition with an approximate range of $\sim 7 \times 10^6 \text{ km}^2$, an area about the size of the United States, and a volume of $\sim 4 \times 10^6 \text{ km}^3$ (Ikanov et al., 2013). Possible kill mechanisms that arose as a result of such intense volcanism include increased $p\text{CO}_2$ (partial pressure of CO_2), ocean anoxia, sub-seafloor methane release, and further continental methane and CO_2 release via ascending basalts into coal beds, evaporites, and carbonates (Knoll et al., 2007). As a result, global cooling followed by warming and oxygen depletion in the oceans occurred (Knoll et al., 2007; Knoll and Fischer, 2011). Estimates of emitted volatiles are as follows: 8.5×10^7 teragrams of CO_2 , 7.0×10^6 teragrams of H_2S , and 6.8×10^7 teragrams of SO_2 (Ogden and Sleep, 2011). It is estimated that $p\text{CO}_2$ during the Permian were 900 times higher than current values (Figure 4) (Knoll et al., 2007)

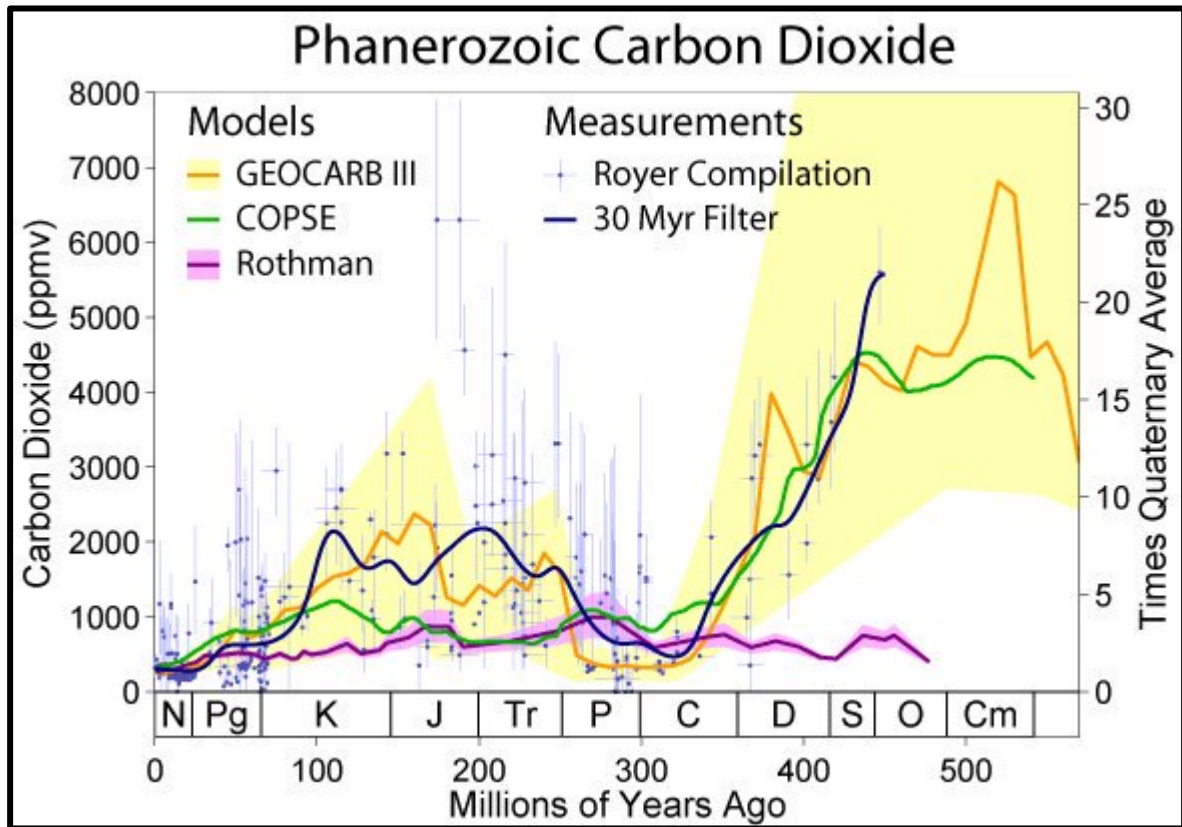


Figure 4. Carbon dioxide values from the present to the Cambrian based off three experimental values. Note the difference in atmospheric concentration between the P-T boundary and the present (Rohde, Robert.
<http://blogs.agu.org/wildwildscience/2009/07/07/new-clue-to-past-co2-levels/>).

A more contemporary kill mechanism proposed by Bottjer et al. (2008) is that of ocean acidification as a result of increased $p\text{CO}_2$. Ocean acidification is the key aspect of this study as its implications are a current and pressing issue. In the context of the late Permian mass extinction, ocean acidification has the potential to explain the detrimental effect on marine, calcifying macro and micro invertebrates as they are dependent upon sensitive oceanic conditions (pH, dissolved oxygen, and nutrient load) for shell formation, reproduction, and metabolism (Knoll et al., 2007; Bond and Grasby, 2016). Moreover, the absence of Triassic reefs and hypercalcifiers/reef builders is further potential evidence of ocean acidification in localities that span the Permian-Triassic boundary (Kershaw et al.,

2012). It is important to realize that the above kill mechanisms most likely acted together in a synergistic fashion which explains the magnitude of extinction in the oceans as well as on land, but ocean acidification poses a unique and more overarching explanation for the taxa of organisms that perished as a result.

In terms of marine organisms, late Permian corals, dasycladacean (green algae), red algae, and calcareous foraminifera all went extinct by the late Triassic while mollusks and chordates remained somewhat resistant with extinctions ranging from ~77% to 0% (Knoll et al., 2007). A synthesis for the mechanisms that allowed specific groups to survive is considered as well as a further discussion regarding the emergence of gastropods in Triassic units of the Nanpanjiang Basin. Furthermore, biologic trends in general include reduced species diversity, decrease in overall size of organisms likely due to increased metabolic rate as $p\text{CO}_2$ levels increased and oceanic oxygen decreased, decrease in richness of skeletal, benthic invertebrates, and reduced bioturbation of sediments well into the middle Triassic which highlights the severity of this event for both marine and terrestrial organisms (Knoll et al., 2007).

A geochemical and faunal succession approach has been used for the Tianwan section to measure not only ecological diversity and dominance but also oceanic conditions at the time of deposition. While paleoecology and geochemical data has been collected throughout the Nanpanjiang Basin, data on the Tian'e platform remains unpublished but can be used to compare its results discussed in this paper to that of other sections published by Lehrmann to ensure a general synthesis can be made in order to understand the intricacies of the late Permian mass extinction (Jin et al., 2000). Research methods include quadrat sampling of both thin sections and hand samples for each representative unit in both sub-sections of the

Tianwan section, analysis of diagenetic structures specifically aragonite fans and stylolites as proposed proxies of ocean acidification, and stable isotope geochemistry analysis of $\delta^{13}\text{C}$ and $\delta^{18}\text{O}$ as parameters of paleoenvironmental change (Heltshe and Forrester, 1985).

The implications of this study pertain to social, economic, political, and environmental issues as the current effects of ocean acidification are at the forefront of climate change research (Turley and Gattuso, 2012). The ocean's chemistry is being altered by carbon dioxide uptake; as CO_2 mixes with the ocean, carbonic acid forms therefore reducing overall pH resulting in ocean acidification. The resulting lowered pH of the ocean has the potential to impact major marine ecosystems and food webs which has substantial implications for the future of the earth (Levin and Le Bris, 2015). Increased anthropogenic carbon dioxide emissions are likely to blame for current ocean acidification. Ocean acidification is believed to be affecting the following: marine systems through dissolution of carbonaceous organisms, societies' dependence upon the ocean for resources, and political policy as global climate change is an issue that affects every single earth-dwelling individual (Turley and Gattuso, 2012). Because Earth's oceans are currently undergoing an ocean acidification event, research into the causes and effects of the Permian-Triassic mass extinction event is pertinent to understanding the implications of our actions. By studying and analyzing stable isotopes, diagenetic structures and processes, and faunal succession and dominance, a better understanding of the mechanics of ocean acidification can be inferred. This understanding is essential for further research into the implications of ocean acidification and ways in which scientists can interpret past events, and how they affected marine and terrestrial organisms. This understanding will aid in the recognition of ways in which mankind can prevent the potential demise of diversity in our oceans. The main

objective of this research is to determine if faunal succession, stable isotope analysis, and diagenetic structures dependent on oceanic conditions in the Tianwan section of the Nanpanjiang Basin provide further evidence for ocean acidification as the cause of the late Permian mass extinction.

METHODOLOGY

Thin sections and hand samples were provided by Dr. D. Lehrmann from Trinity University in San Antonio, Texas, from a 2011 trip to the Nanpanjiang Basin. The hand samples were collected from two subsections along a road-cut along the Tianwan section in the Tian'e platform (Figure 2). Both subsections span the Permian-Triassic units and are simply laterally continuous units divided only by distance. Thin sections were prepared by Quality Thin Sections.

Twenty-one thin sections from the Tainwan section (ten from subsection 1 and eleven from subsection 2) were examined using a reflecting microscope at 40x magnification (Figure 5). Using the quadrat sampling method, random but systematic collection of faunal succession data was completed by placing an overlay with a 1.5 centimeter diameter viewing circle on top of each thin section in five different places and point counting the number of macro and micro invertebrates including pelagic foraminifera, crinoids, gastropods, bryozoan, brachiopod, ostracods, sphinctozoans, calcispheres, dasycladaceans, algae, fusulinids, and clastic carbonaceous grains (Figures 5 and 6). Five quadrat sample locations were used for each thin section to ensure accuracy of both data and the sample size. The quadrat sampling method is used specifically by ecologists to quantify population size of sessile organisms for a given community; data is collected from a small area to represent the whole (Heltshe and Forrester, 1985). Rather than point count using a grid of the entire thin section, which is traditionally used in paleontology studies, quadrat sampling was used to eliminate bias as it is random and every member of the population has a chance of being counted (Rego et al., 2012). Additionally, quadrat sampling preserves the structure of taxa

dominance versus diversity of the community, a critical component to understanding paleoecology during mass extinctions (Heltshe and Forrester, 1985).

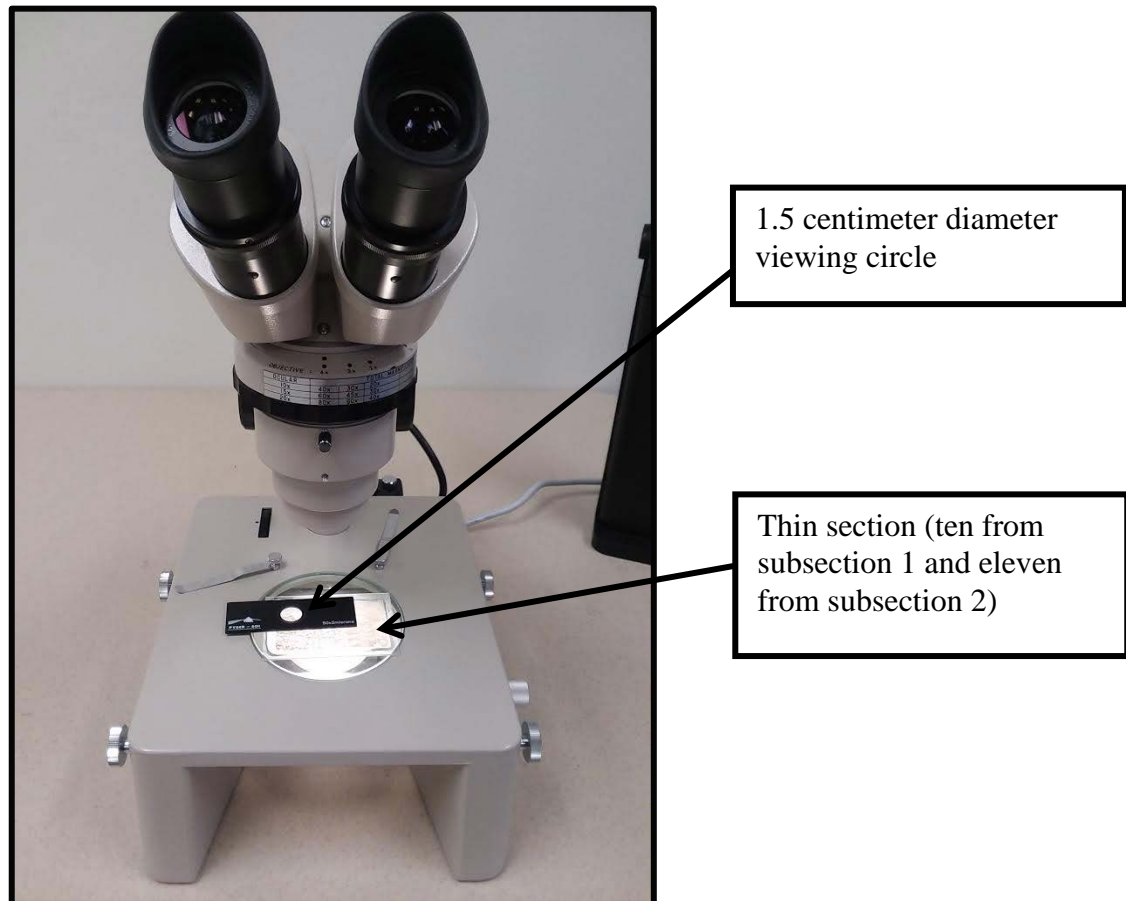


Figure 5. Quadrat sampling method of point counting to quantify diversity and dominance of twenty-one thin section (ten from subsection 1 and eleven from subsection 2).

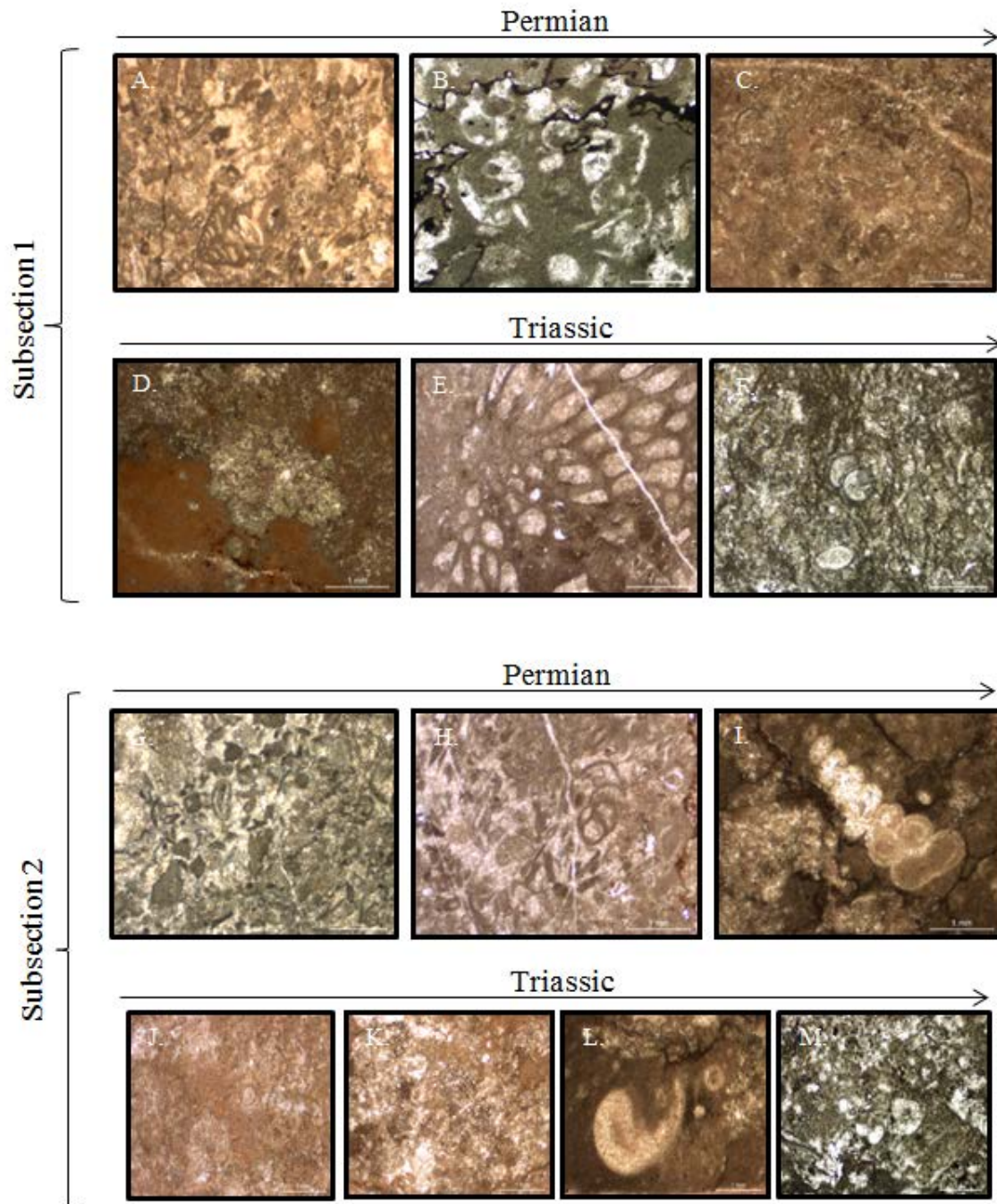


Figure 6. Examples of fossils spanning the Permian (skeletal packstone) –Triassic (microbial boundstone) from both sub sections of the Tianwan section. A) foraminifera, spinozoan, and additional fragmented fossils B) gastropods C) ostracods D) microbial fabric and micrite fill post extinction E) bryozoan F) calcispheres within microbialite fabric G) foraminifera and fusulinid fragmented fabric H) further foraminifera fabric I) pelagic foraminifera J) scant fragmented fossils within microbial fabric K) microbial fabric L) gastropod M) microbial fabric with a crinoid present. Trends for both subsections are increased fauna in Permian units to microbial fabrics and scant fauna in the Triassic units.

Using faunal succession data (number of macro and micro invertebrates in order according to appearance in the rock record), Simpson's Index and Simpson's Index of Diversity were calculated to quantify species diversity (number of different species in a community) and dominance (the magnitude to which a species is more plentiful than its competitors) (Whittaker, 1965). It is important to note that point counting using the quadrat sampling method was not completed at the species level as the amount of time and resources was limited for the depth of this project. Instead, taxa of organisms were counted based on the types of the micro and macro invertebrates (Figure 6). The equations are as follows (Whittaker, 1965):

- Simpson's Index: $D = \frac{\sum n(n-1)}{N(N-1)}$
- Simpson's Index of Diversity: $1 - D$

Where:

- D is Simpson's Index which quantifies diversity of a specific sample; the greater the number (between 0 and 1), the lower the diversity (Simpson, 1949).
- n is the total number of organisms of a particular taxa
- N is the total number of organisms of all types
- Simpson's Index of Diversity gives the dominance of organisms of a specific sample size; the greater the number (between 0 and 1), the greater the dominance.

Simpson's Index measures the probability that two individual fossils randomly selected from a sample will belong to the same taxa by taking into account both species richness and evenness. However, Simpson's Index alone does not prove useful when

quantifying the faunal succession from before, during, and after the Permian-Triassic mass extinction as dominance must be taken into account rather than just diversity; this principle is explained by the term “disaster taxa” (Correa and Baker, 2011). Disaster taxa are opportunistic genera that dominate a community post natural disaster or extinction and in the case of the late Permian mass extinction, mollusks, brachiopods, and vertebrates serve as dominant, disaster taxa (Twitchett et al., 2004). By quantifying the dominance of disaster taxa, a more general understanding of the severity and conditions of the late Permian mass extinction can be made. Moreover, Simpson’s Index of Diversity quantifies dominance of taxa as their presence indicates changes at the ecological level. These observed changes are the most useful when representing mass extinctions and their effects in a specific community (Whittaker, 1965; Droser et al., 2000) quadrat sampling has not traditionally been used for mass extinctions and moreover, when used for mass extinctions, it was used by DiMichele et al. (2001) for flora making quadrat sampling of late Permian Tianwan carbonate deposits a multidisciplinary and contemporary approach never before recorded.

Shannon’s Index was used as an additional method to quantify diversity to take into account the entropy or uncertainty of the specific environment/community. Entropy is explained by attempting to characterize the “unpredictability” or randomness between two random variables (in this case, differing taxa) (Gorelick, 2006). The equation is as follows:

- Shannon’s Index: $H = -\sum_{i=1}^S p_i \ln p_i$

Where:

- H is Shannon’s Diversity Index where the greater the number (between 0 and ∞), the greater the diversity (Shannon, 1948)
- R is the total number of taxa in the given community

- p_i is proportion of S made up of the i th species (randomness or “unpredictability”)

The data collected using Shannon’s Index can be contrasted to Simpson’s Index values which mitigate the limitations of point counting by taxa and not by species as entropy/uncertainty is taken into account (Whittaker, 1965).

The observed emergence of gastropods in the Triassic Tianwan samples is an additional key and understudied aspect of faunal succession across the late Permian mass extinction specifically in the Tian’e platform. Using the reflecting microscope, thin sections, and polished slabs, the numbers of gastropods were quantified up-section and their morphology was catalogued.

All marine organisms counted were grouped into hypercalcifiers, moderate calcifiers, and non-calcifiers to further define the mechanisms of extinction during the late Permian. Knoll et al. (2007) define hypercalcifiers as 1) “animals with a calcium carbonate skeleton that was massive with respect to supporting living organic tissue and formed from fluids minimally buffered by physiology” 2) moderate calcifiers as “animals with a calcium carbonate skeleton of moderate mass with respect to living organic tissue and formed from fluids that are relatively well buffered with respect to the factors that govern carbonate precipitation” and non-calcifiers as 3) “animals with skeletons made of materials other than calcium carbonate or with minimal, internal calcium carbonate spicules not used for mechanical support.” No non-calcifiers were found using the quadrat sampling method in this study but conodont (non-calcifiers) richness are documented to have recovered and boomed post extinction (Chen et al., 2009; Petsios and Bottjer, 2016).

$\delta^{13}\text{C}$ and $\delta^{18}\text{O}$ stable isotopes were collected and analyzed from before, during, and after the late Permian mass extinction from both subsections of the Tianwan section to determine paleoenvironmental conditions as well as the extent of diagenesis (either meteoric or marine).

- a. 100 mg of bulk carbonate from six samples (three from each subsection within the Tianwan section) was collected to represent before, during, and after the late Permian mass extinction for $\delta^{13}\text{C}$ and $\delta^{18}\text{O}$ stable isotope analysis.
- b. Samples were sent to Isotech Laboratories for $\delta^{13}\text{C}$ and $\delta^{18}\text{O}$ stable isotope analysis.
- c. Stable isotope data was compared to its respective location along the Tianwan section as well as to existing data of additional sections completed by Lehrmann et al. (2015).

A brief literature review of additional stable isotopes not utilized in this study will be summarized in the Future Work section as they are critical to the understanding of the mechanisms of the late Permian mass extinction.

Twenty-one thin sections were examined using a reflected light microscope. Hand sample slabs were observed for locations of diagenetic structures such as stylolites (pressure-dissolution structures as a result of burial) and aragonite fans (believed to be the result of ocean acidification) (Greene et al., 2012). Analysis of diagenetic structures will not have a quantitative data component, but instead is a working hypothesis of new proxies for paleo-ocean acidification.

RESULTS

Faunal Succession: Tianwan subsection 1 and 2

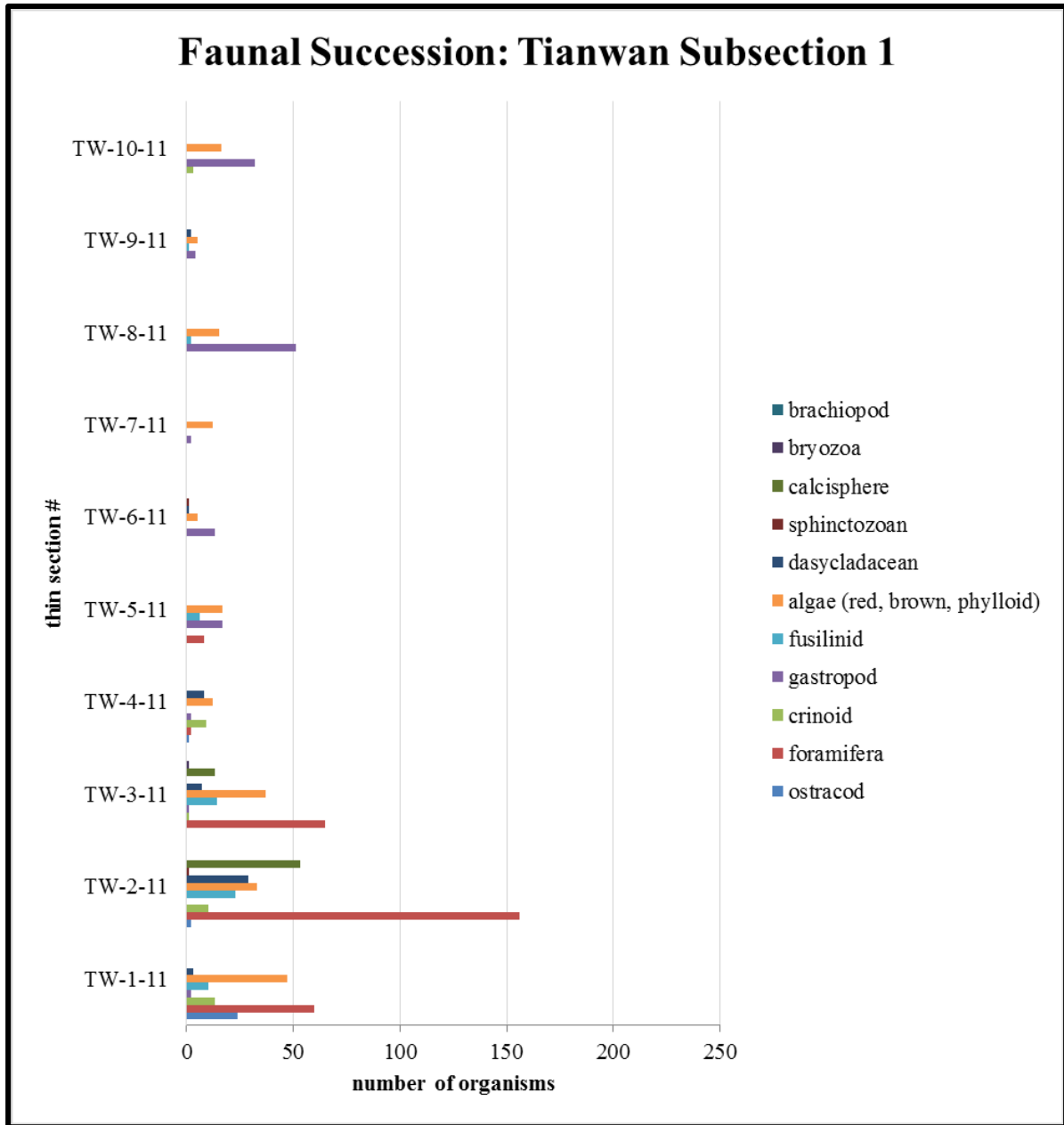


Figure 7. Faunal succession of the first subsection of the Tianwan section. The late Permian mass extinction is indicated by the dashed, red line with Permian at the bottom and Triassic at the top. Note the dramatic decrease in abundance of organisms post extinction as well as the emergence of gastropods in TW-5-11 into TW-10-11.

Figure 7 shows the faunal succession of eleven taxa of marine macro and microorganisms in subsection 1 of the Tianwan section. Figure 7 shows a trend of increased taxa abundance until thin section TW-4-11 (the extinction boundary is between TW-3-11 and TW-4-11) where taxa abundance decreases. In terms of evenness, the abundance of taxa decreases up section meaning fewer taxa are more prominent signifying they dominate the section post extinction. Additionally, gastropods emerge in sample 5 and dominate into sample 10.

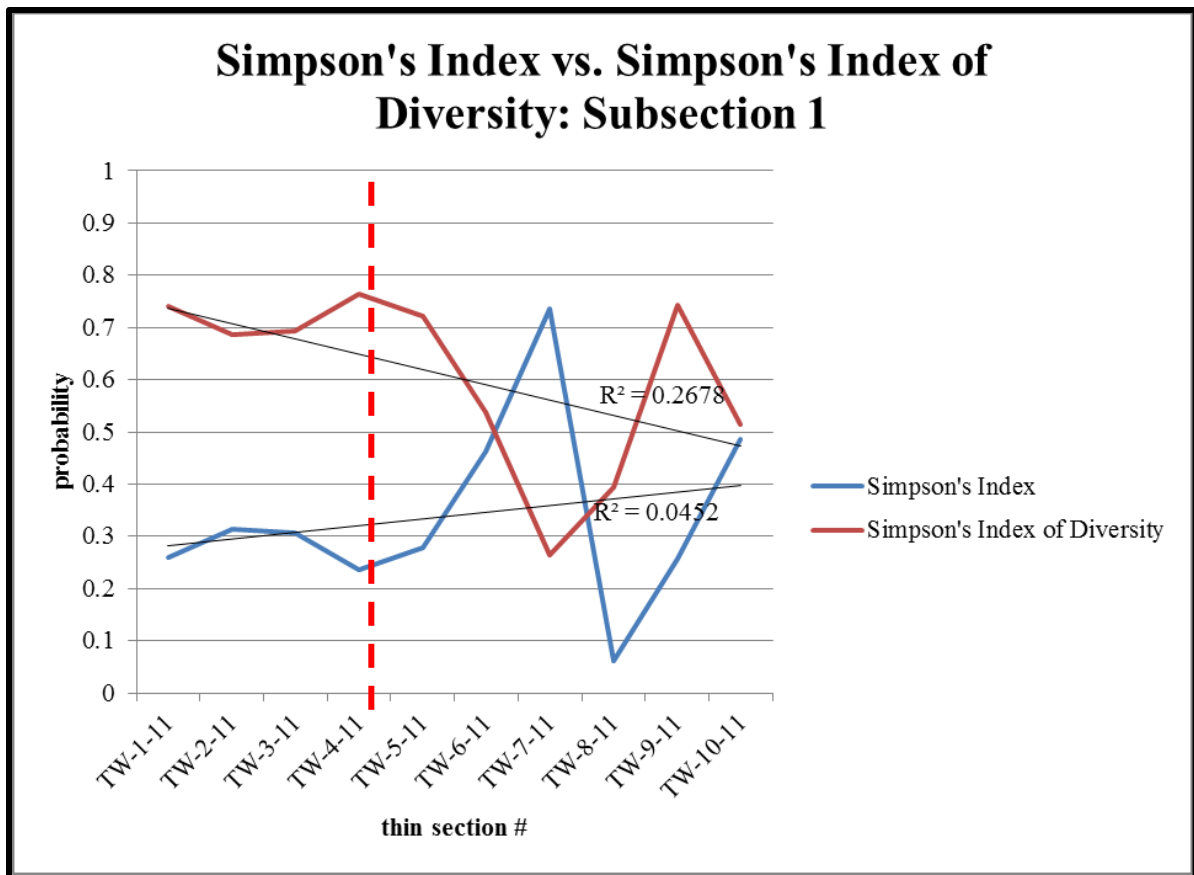


Figure 8. Simpson's Index (in blue) vs. Simpson's Index of Diversity (in red). Note the erratic cyclicality of both graphs post late Permian mass extinction indicated by the dashed red line with Permian to the left and Triassic to the right of the dashed line. The erratic nature suggests chaos within the biological community post extinction.

Figure 8 shows the Simpson's Index versus Simpson's Index of Diversity for subsection 1 of the Tianwan section. Simpson's Index shows a general positive trend

meaning the samples are more diverse up section (into the Triassic). While it would not be expected to increase in diversity, the positive trend inaccurately represents the diversity of subsection 1 due to the erratic nature of the graph. Moreover, the R-squared value for Simpson's Index is 0.0452 which is lower than the statistically significant value of 0.6 meaning the values do not correlate to the line of best fit (trend line in Figure 8). However, it is not expected that mass extinctions have an R-squared value that is statistically significant as mass extinctions create irregular patterns of diversity (Figure 8). The dramatic ebbs and flows of Simpson's Index suggest erratic changes in not only the abundance of organisms but also the community.

In the case of Simpson's Index of Diversity for subsection 1, the trend is negative meaning less taxa dominate the samples up section (into the Triassic) (Figure 8). Similarly to Simpson's Index for the first subsection, a decrease in taxa dominance post extinction would not be expected, but the trend inaccurately represents dominance due to the erratic nature of the graph. The R-squared value for the Dominance Index is 0.2678 which is lower than the statistically significant value of 0.6 meaning the values do not correlate to the line of best fit (trend line). However, as with Simpson's Index, mass extinctions are not expected to have an R-squared value that is statistically significant because mass extinctions create irregular patterns of taxa dominance (Figure 8). The chaotic cyclicity suggests dramatic changes in taxa dominance and the community as a result of the late Permian mass extinction.

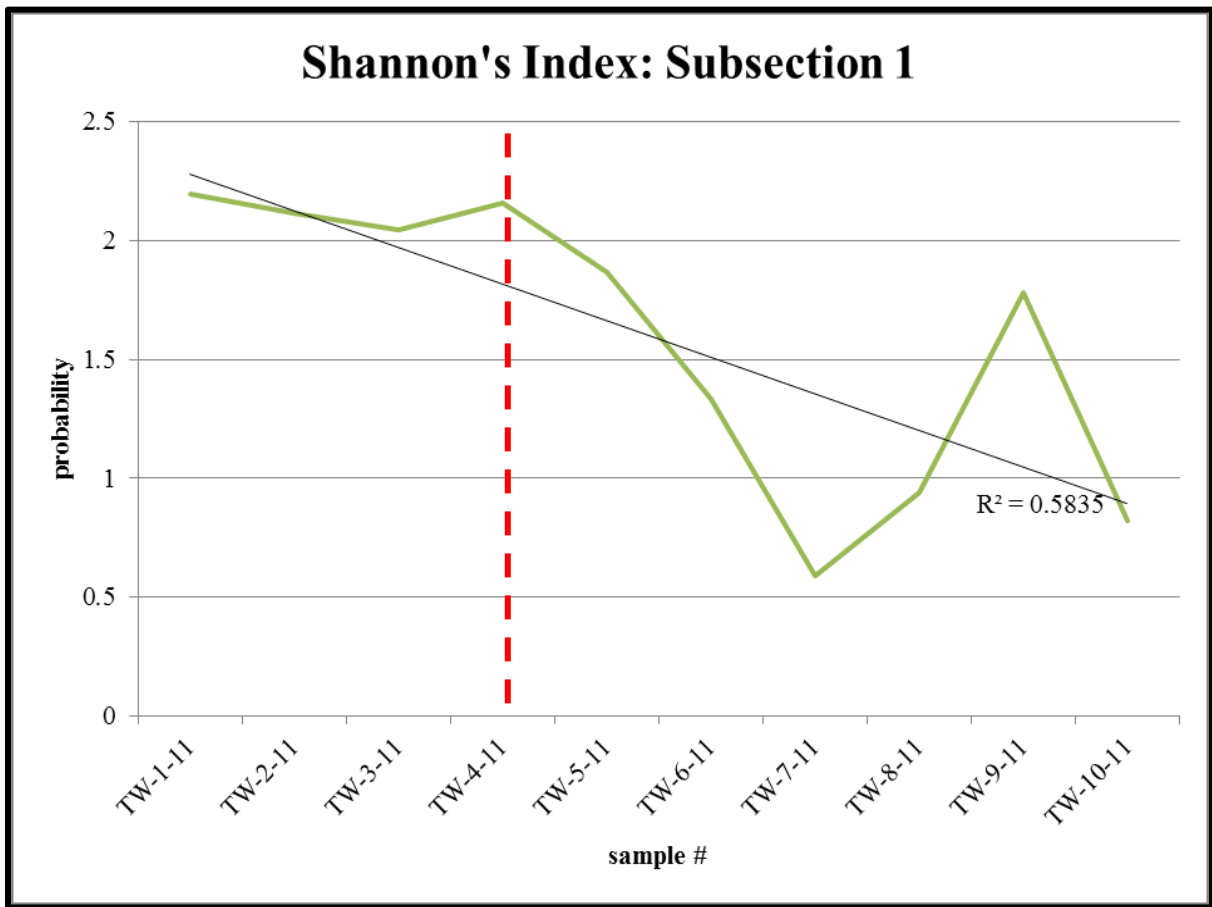


Figure 9. Shannon's Index for the first subsection of the Tianwan section which is an additional method of quantifying diversity but takes into account the chaos of the community. Note the overall negative trend and dramatic decrease in diversity post extinction indicated by the dashed red line (Permian to the left and Triassic to the right).

Figure 9 shows Shannon's Index for subsection 1 of the Tianwan section. This is an additional method of quantifying diversity that takes into account the chaos of the community. The overall trend is negative meaning that diversity decreases up-section into the Triassic units which is what we would expect when dealing with a mass extinction. The R-squared value is 0.5835 meaning the values do not correlate to the line of best fit but only by a margin of 0.0265. Shannon's Index more accurately represents diversity for the first subsection in comparison to Simpson's Index as it accounts for the chaos of the community (Figure 8 and 9).

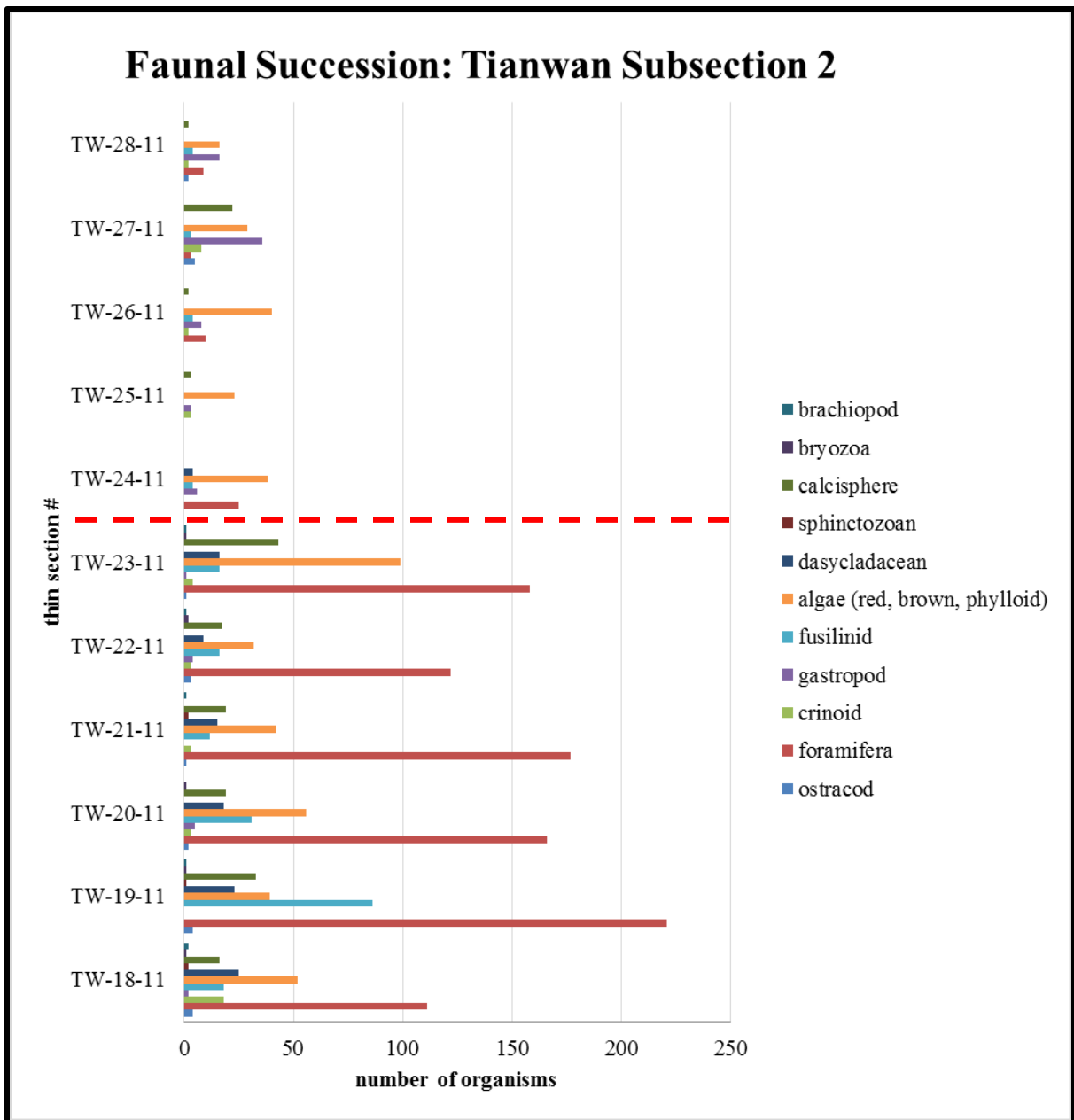


Figure 10. Faunal succession of the second subsection of the Tianwan section. The late Permian mass extinction is indicated by the dashed, red line with Permian at the bottom and Triassic at the top. Note the dramatic decrease in abundance of organisms post extinction as well as the emergence of gastropods in TW-24-11 to TW-28-11.

Figure 10 shows the faunal succession of eleven taxa of marine macro and microorganisms in subsection 2 of the Tianwan section. The graph shows a trend of increased taxa abundance until thin section TW-24-11 (the extinction boundary is between thin section TW-23-11 and thin section TW-24-11) where the abundance of taxa dramatically decreases. In terms of evenness, the abundance of taxa decreases up section meaning fewer taxa are more prominent signifying they dominate the section post extinction. Moreover, gastropods emerge in thin section TW-24-11 and dominate into thin section TW-28-11.

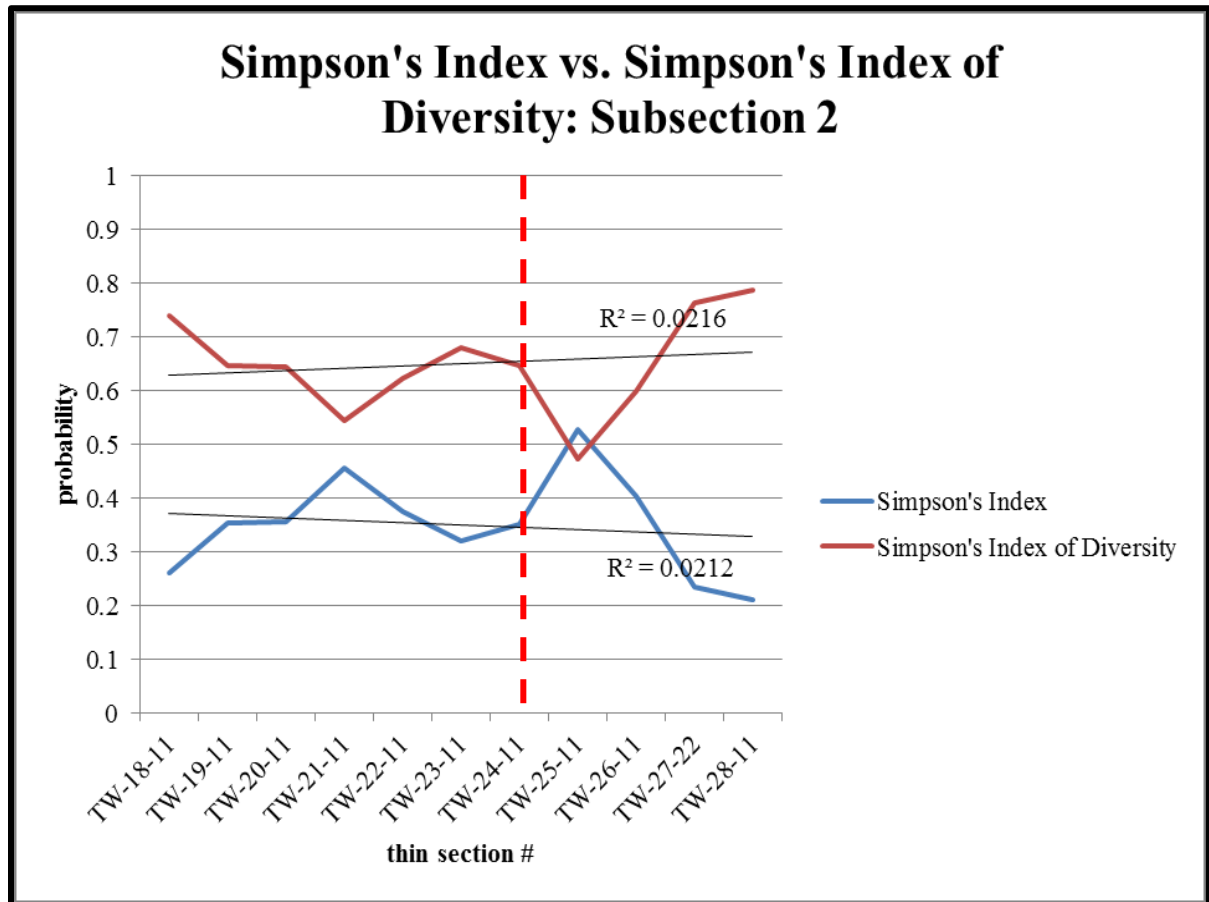


Figure 11. Simpson's Index (in blue) vs. Simpson's Index of Diversity (in red). Note the erratic cyclicality of both graphs post late Permian mass extinction indicated by the dashed red line with Permian to the left and Triassic to the right of the dashed line. The erratic nature suggests chaos within the biological community post extinction.

Figure 11 shows the Simpson's Index versus Simpson's Index of Diversity for subsection 2 of the Tianwan section. Simpson's Index shows a general negative trend meaning there is a lower diversity of taxa up section (into the Triassic). A decrease in diversity is what we would expect as the result of the late Permian mass extinction, but it is important to note the erratic nature of the graph best represented by the low R-squared value. The R-squared value for Simpson's Index is 0.0212 which is lower than the statistically significant value of 0.6 meaning the values do not correlate to the line of best fit (trend line in Figure 11). However, mass extinctions are not expected to have an R-squared value that is statistically significant as mass extinctions create irregular patterns of diversity (Figure 11). The dramatic ebbs and flows of Simpson's Index suggest erratic changes in not only the abundance of organisms but also the community itself as a result of the late Permian mass extinction.

In the case of Simpson's Index of Diversity for subsection 2, the trend is positive meaning fewer taxa dominate the samples up section (into the Triassic) (Figure 11). Similarly to Simpson's Index for the second subsection, we would expect an increase in taxa dominance post extinction, but it is important to note the erratic nature of the graph represented by the low R-squared value. The R-squared value for the Dominance Index is 0.216 which is lower than the statistically significant value of 0.6 meaning the values do not correlate to the line of best fit (trend line). However, as with Simpson's Index, we do not expect mass extinctions to have an R-squared value that is statistically significant because mass extinctions create irregular patterns of dominant taxa (Figure 11). The chaotic cyclicity suggests dramatic changes in taxa dominance and the community as a result of the late Permian mass extinction.

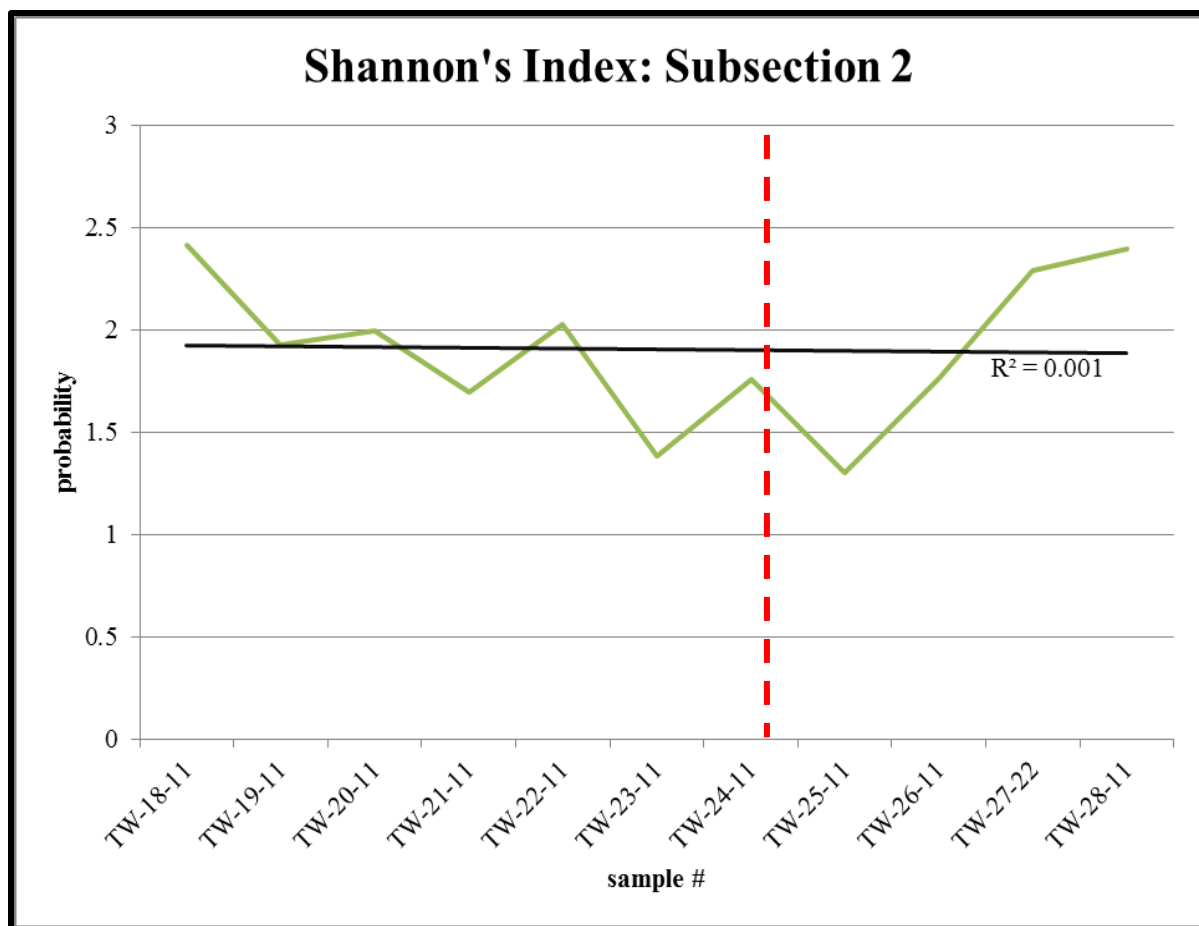


Figure 12. Shannon's Index for the first subsection of the Tianwan section which is an additional method of quantifying diversity but takes into account the chaos of the community. Note the overall negative trend and dramatic decrease in diversity post extinction indicated by the dashed red line (Permian to the left and Triassic to the right).

Figure 12 shows Shannon's Index for subsection 2 of the Tianwan section. The overall trend is slightly negative meaning that diversity decreases up-section into the Triassic units which is what we would expect when dealing with a mass extinction. The R-squared value is 0.001 meaning the values do not correlate to the line of best fit. Shannon's Index more accurately represents diversity for the first subsection in comparison to Simpson's Index as it accounts for the chaos of the community (Figure 11 and 12).

Stable Isotope Geochemistry

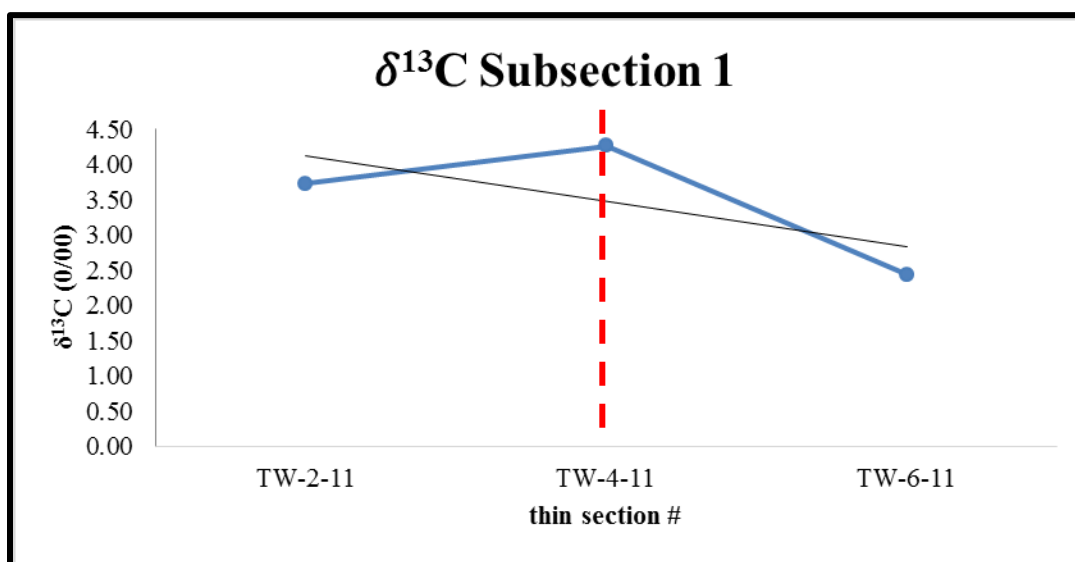


Figure 13. $\delta^{13}\text{C}$ values across the late Permian mass extinction indicated by the dashed red line (Permian is to the left and Triassic is to the right). The initial trend before the mass extinction is positive while the trend post extinction is negative. Overall, the trend is negative indicated by the trend line.

Figure 13 shows the bulk carbonate $\delta^{13}\text{C}$ stable isotope values from samples taken before, during, and after the late Permian mass extinction respectively of subsection 1. The excursion value (numerical difference between samples) between TW-2-11 and TW-4-11 is 0.53 ‰ (Figure 13). The excursion value between TW-4-11 and TW-6-11 is -1.33 ‰ (Figure 13). The overall trend for $\delta^{13}\text{C}$ is negative as the value decreased into the Triassic units (TW-6-11).

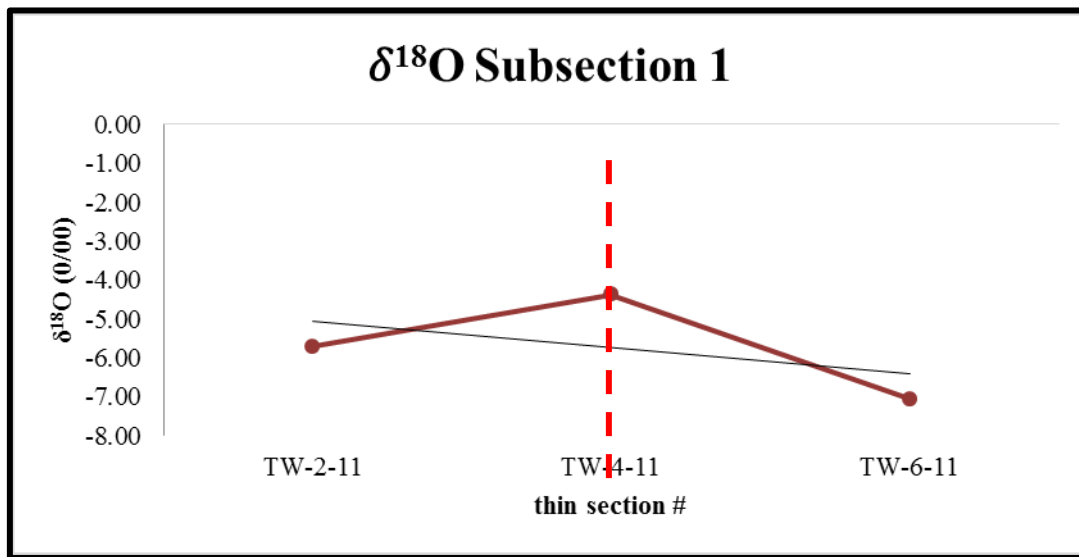


Figure 14. $\delta^{18}\text{O}$ values across the late Permian mass extinction indicated by the dashed red line (Permian is to the left and Triassic is to the right). The initial trend before the mass extinction is positive while the trend post extinction is negative. Overall, the trend is negative indicated by the trend line.

Figure 14 shows bulk carbonate $\delta^{18}\text{O}$ stable isotope values from samples taken from before, during, and after the late Permian mass extinction respectively for subsection 1. The excursion between TW-2-11 and TW-4-11 is 1.33 ‰ (Figure 13). The excursion between TW-4-11 and TW-6-11 is -2.68 ‰ (Figure 13). The overall trend for $\delta^{18}\text{O}$ is negative as the values decrease into the Triassic units (TW-6-11).

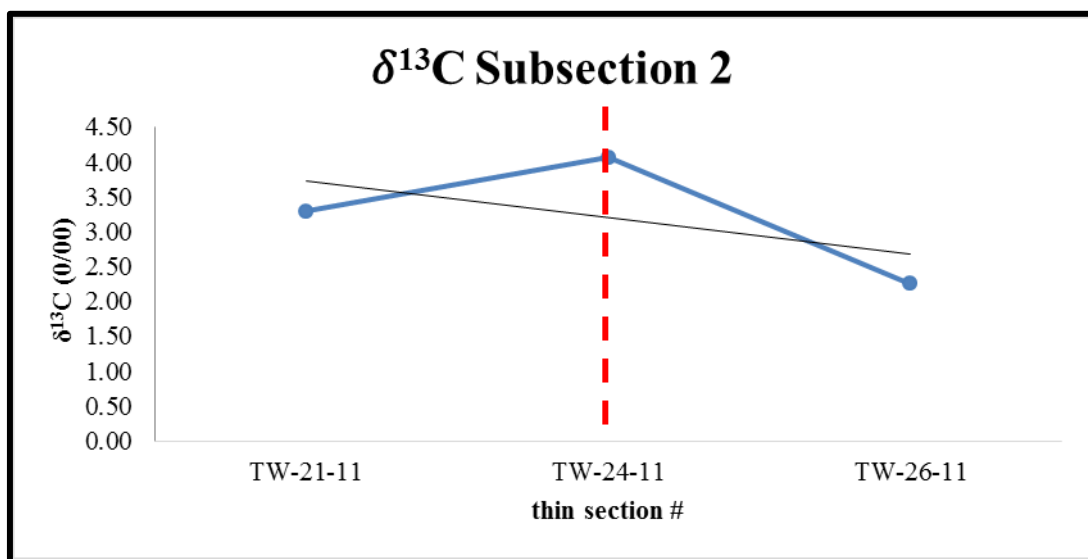


Figure 15. $\delta^{13}\text{C}$ values across the late Permian mass extinction indicated by the dashed red line (Permian is to the left and Triassic is to the right). The initial trend before the mass extinction is positive while the trend post extinction is negative. Overall, the trend is negative indicated by the trend line.

Figure 15 shows the bulk carbonate $\delta^{13}\text{C}$ stable isotope values from samples taken from before, during, and after the late Permian mass extinction respectively for subsection 2. The excursion value between TW-21-11 and TW-24-11 is 0.78 ‰ (Figure 15). The excursion value between TW-24-11 and TW-26-11 is -1.82 ‰ (Figure 15). The overall trend is negative and the values decrease into the Triassic units (TW-26-11) much like the first subsection values.

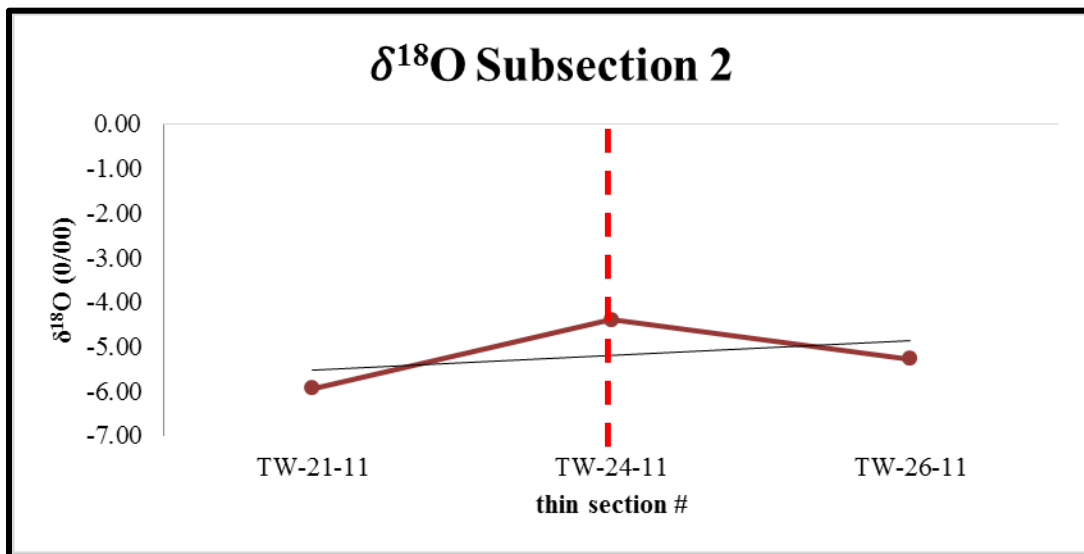


Figure 16. $\delta^{18}\text{O}$ values across the late Permian mass extinction indicated by the dashed red line (Permian is to the left and Triassic is to the right). The initial trend before the mass extinction is positive while the trend post extinction is negative. Overall, the trend is negative indicated by the trend line.

Figure 16 shows the bulk carbonate $\delta^{18}\text{O}$ stable isotope values from samples taken from the before, during, and after the late Permian mass extinction respectively for subsection 2. The excursion value between TW-21-11 and TW-24-11 is 1.55 ‰ (Figure 16). The excursion value between TW-24-11 and TW-26-11 is -0.88 ‰ (Figure 16). The overall trend is slightly positive, but the values decrease into the Triassic units (TW-26-11).

Diagenetic Structures

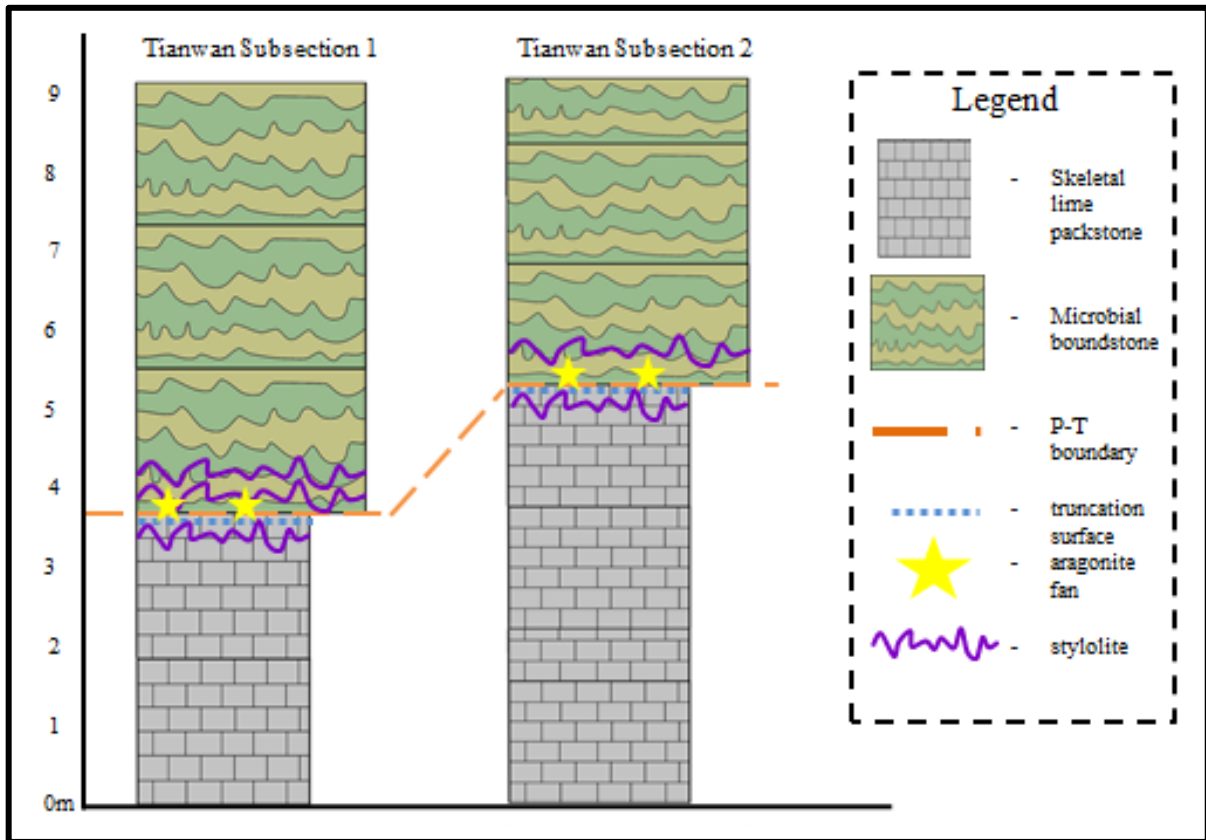


Figure 17. Diagenetic structures from both subsections of the Tianwan section. The dashed orange line indicated the Permian-Triassic boundary. Note the location of aragonite fans and stylolites in respect to the location of the truncation surface and extinction boundary.

Figure 17 shows the location of diagenetic structures (aragonite fans and stylolites) in both subsections of the Tianwan section. Of particular importance is the location of the diagenetic structures in respect to the truncation surface (dashed blue line) and mass extinction boundary (dashed orange line) (Figure 17). The diagenetic structures are centralized along the truncation surface and mass extinction boundary. It is important to note that there is not a quantitative component to the diagenetic structures, only their location along the stratigraphic column in both subsections (Figure 13).

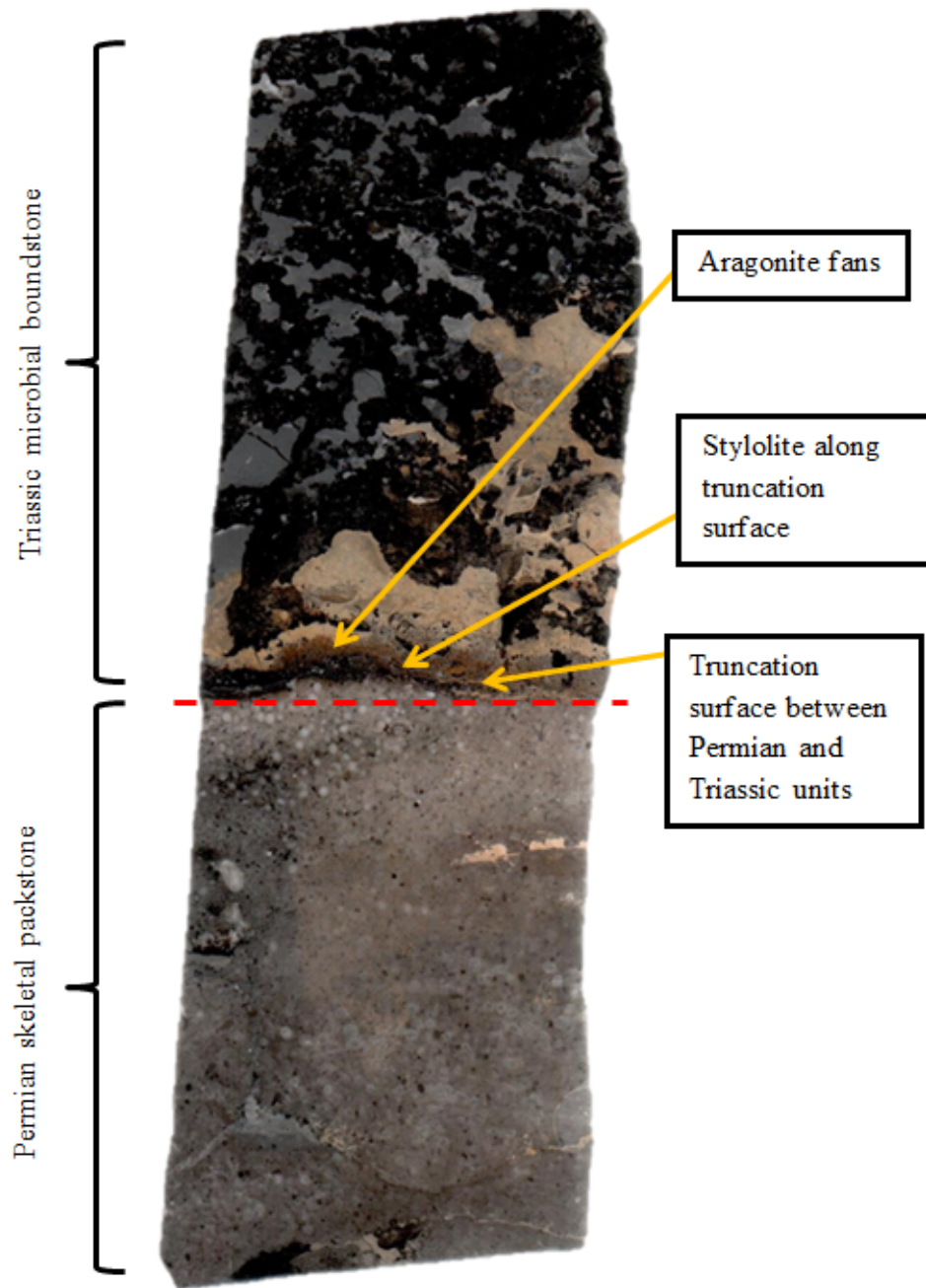


Figure 18. The late Permian mass extinction boundary indicated by the dashed red line. Note the difference in fabric between the Permian and Triassic units.

Figure 18 shows a polished slab of the late Permian mass extinction boundary. Of particular interest is the location of stylolites and aragonite fans in respect to the extinction

boundary and truncation surface. The aragonite fans propagate along the truncation surface in the Triassic microbial boundstone units.

DISCUSSION

Faunal Succession and Dominance: The faunal succession data collected shows a dramatic drop in the abundance of taxa for both subsections of the Tianwan section. For both subsections, hypercalcifiers flourished (foraminifera, brachiopods, bryozoan, crinoids, ostracods, and sphinctozoans) during the late Permian (thin sections TW-1-11 through TW-3-11 for subsection 1 and thin sections TW-18-11 through TW-23-11 for subsection 2) (Knoll et al., 2007). Furthermore, the faunal succession accurately shows the rapidity and severity expected from the late Permian mass extinction. In thin sections TW-3-11 and TW-4-11 (pre mass extinction) 8 and 6 taxa were counted respectively while in thin section TW-5-11 (early Triassic or post mass extinction), only four total taxa were counted. Similarly, taxa from TW-21-11 through TW-23-1 (pre mass extinction) of subsection 2 has nine, ten, and ten taxa counted respectively while in TW-24-11 through TW-28-11 (post mass extinction), five, four, six, seven, and seven taxa were counted respectively.

It is clear from Figures 7 and 10 that the faunal succession accurately matches what is to be expected from a mass extinction event—major loss in abundance and a decline in the number of individual taxa post extinction, especially that of hypercalcifiers, if ocean acidification is to be invoked. Post extinction, only gastropods, algae and a few (values ranged from 0 to 8 individuals) forams as well as sponges (sphinctozoans) and crinoids remained, meaning moderate calcifiers dominated the community in the early Triassic.

By recognizing that hypercalcifiers were most heavily affected, not only in the Tianwan section but the Late Permian mass extinction as a whole, ocean acidification proves to be the most probable cause of extinction as hypercalcifiers are physiologically not able to buffer carbonate fluids as a result of hypercapnia (excess CO₂) in acidic conditions (Kershaw

et al., 2012). Thus data from the Tianwan section supports ocean acidification as a probable kill mechanism for marine organisms based on faunal succession of different calcifiers.

An interesting observation is that of the emergence and dominance of gastropods post extinction. This observation fits the moderate calcifier description of organisms being able to withstand ocean acidification and its accompanying effects (Knoll and Fischer, 2011).

Because gastropods are better able to buffer calcifying fluids due to their metabolism and complex morphology, it is not surprising that they filled niches and survived by approximately 42.4% overall post extinction (Knoll and Fischer, 2011; Knoll et al., 2007).

Because of these traits, gastropods serve as the disaster taxa for the Tianwan locality (Peters and Bottjer, 2016). In order to understand Permian/Triassic gastropod's morphology, a synthesis of modern gastropods living in acidic conditions must be made and compared to both Permian and Triassic gastropods. Additionally, it is the hope of this thesis that stable isotope geochemistry can be performed in the future on the shells of gastropods before and after extinction as the composition of their shell potentially changed in response to lowered pH (Capdevielle, n.d.).

In respect to Simpson's Index and Simpson's Index of Diversity values for subsection 1 of the Tianwan section illustrated by Figure 8, a trend line was applied to both graphs to show either positive or negative general trends. Simpson's Index had a positive trend overall implying diversity increased post extinction into the Triassic Period, and Simpson's Index of Diversity showed a general negative trend implying dominance decreased. This trend does not necessarily make sense as one would expect that diversity would decrease and dominance would increase. Rather than focus on the general trend of both Simpson's Index and Simpson's Index of Diversity, it is important to consider chaotic cyclicity between each thin

section. TW-1-11 through TW-3-11 (pre mass extinction) show little variance between probability values, but TW-4-11 through TW-10-11 (post extinction) show sharp rises and falls suggesting erratic changes in the abundance of taxa and the community. The R-squared values for both Simpson' Index and Simpson's Index of Diversity were 0.0452 and 0.2678 respectively, but it can be argued that R-squared values should not be accepted as definitive proof of statistical insignificance as values for Simpson's Index and Simpson's Index of Diversity are irregular and display the irregularity and severity of a mass extinction. Mass extinctions do not follow an expected ecological trend, especially in regards to the end Permian, thus it is not surprising to see these types of changes. The end Permian mass extinction, as stated previously, acted with swiftness and magnificent force. Figures 8 and 11 outline that force clearly as values are not steady and change dramatically once the extinction occurred.

As a way to mitigate the irregularity of Simpson's Index and Simpson's Index of Diversity trends, Shannon's Index takes into account the "entropy" or chaos accompanying ecological events and uses it as an aspect of its equation. Shannon's Diversity Index for both subsections is negative in terms of its trend. This negative trend for Shannon's Index indicates that diversity decreased post extinction which fits the expected mass extinction trend (Jin et al., 2000). The R-squared values (0.5835 for subsection 1 and 0.001 for subsection 2) for Shannon's Index are considered insignificant as they are both below 0.6, but more sampling from the Tianwan section of the Tian'e platform must be completed in the future to ensure statistical significance.

The scope of this research remains small; more sampling is needed from multiple localities in the Tianwan section to ensure statistical values can be accepted. However, for

the purpose of this study and for understanding the kill mechanisms (specifically ocean acidification) of the late Permian mass extinction, faunal succession as well as the chaotic cyclicity of both Simpson's Index and Simpson's Index of Diversity values shed the most light on the late Permian mass extinction.

Stable Isotopes: An isotope is an atom whose nuclei contain the same number of protons but a different number of neutrons. Stable isotopes, unlike their unstable counterparts are not radioactive. Many light elements such as carbon and oxygen have different proportions of at least two isotopes. The heavier of the two usually reacts more slowly. The difference in the reaction rates results in different isotope ratios in the resultant material (International Atomic Energy Agency, 2017). Biological processes known as vital effects and changes in temperature and climate (e.g. more arid versus more humid) can result in fractionation of these stable isotopes. Knowing how these processes affect the isotopic ratios allows the interpretation of ancient environments with respect to biological activity and climate (International Atomic Energy Agency, 2017). An important facet to understanding stable isotope values from both subsections of the Tianwan section is that three main processes constrain carbonate systems; CO₂ from earth sources, chemical weathering of silicate minerals, and carbonate mineral precipitation (Knoll and Fischer, 2011). These constraints are taken into account when analyzing both $\delta^{13}\text{C}$ and $\delta^{18}\text{O}$ to ensure variabilities are considered and quantified.

$\delta^{18}\text{O}$ is influenced by three major variables: water temperature, variations in global ice volume, and mineral precipitates (opal or calcite) (Maslin and Swann, 2006). The ratio between $\delta^{18}\text{O}$ and $\delta^{16}\text{O}$ reveals paleoclimatology conditions because the heavier $\delta^{18}\text{O}$ goes into the ocean during periods of warming while the lighter $\delta^{16}\text{O}$ is trapped in ice during

cooling periods (Maslin and Swann, 2006). $\delta^{18}\text{O}$ data for subsection 1 shows a negative overall trend while the trend for subsection 2 is slightly positive. However, deciphering excursion values between each sample proves more useful when determining paleo environmental conditions. For subsection 1, the excursion value between TW-2-11 and TW-4-11 (Figure 14, before and during extinction) is 1.33 ‰ which suggests a general decrease in global temperature. Conversely, between TW-4-11 and TW-6-11 (Figure 14, during and after extinction) the excursion value is -2.68 ‰ suggesting the temperature begins to rise and warms (Maslin and Swann, 2006). For the subsection 2, the excursion between TW-21-11 and TW-24-11 (Figure 16, before and during extinction) the excursion value is 1.55 ‰ suggesting a decrease in global temperature, but between TW-24-11 and TW-26-11 (Figure 16, during and after extinction) the excursion value is -0.88 ‰ suggesting a global average temperature increase and warming period. Both subsections show a very similar trend of cooling then warming. The decrease of global average temperature pre extinction is explained by the hypothesis of the emplacement of the Siberian Traps igneous province as global average temperatures would have decreased as a result initially but warmed post-extinction. Moreover, an increase in global average temperature post extinction correlates to literature that states the earth entered a global warming phase post mass extinction (Bond and Grasby, 2016).

$\delta^{13}\text{C}$ reflects ocean productivity, ocean circulation, and storage of carbon in organic material through the ratio of $\delta^{13}\text{C}$ and $\delta^{12}\text{C}$. $\delta^{12}\text{C}$ is lighter and therefore more favored by organisms leaving $\delta^{13}\text{C}$ in the water as an indicator of primary productivity and oceanic mixing (Maslin and Swann, 2006). $\delta^{13}\text{C}$ data for both subsections shows a general negative trend (Figures 13 and 15). However, deciphering excursion values between each sample is

more useful in this case. For TW-2-11 and TW-4-11 (Figure 13, before and during extinction) the excursion value is 0.53 ‰ indicating increased CO₂ and higher primary productivity. The excursion value between TW-4-11 and TW-6-11 (Figure 13, during and after extinction) is -1.33 ‰ indicating decreased primary productivity and CO₂. For subsection 2 the excursion value between TW-21-11 and TW-24-11 (Figure 15, before and during extinction) is 0.78 ‰ indicating increased CO₂ and increased primary productivity. The excursion value between TW-24-11 and TW-26-11 (Figure 15, during and after extinction) is -1.82 ‰ indicating decreased CO₂ levels as well as primary productivity. The increase in CO₂ in both subsections before the late Permian mass extinction is likely due to the emplacement of the Siberian Traps igneous province releasing large amounts of volatiles (specifically CO₂) into the atmosphere which were then dissolved into the ocean (Knoll et al., 2007). After the mass extinction, CO₂ levels decreased which fits the current atmospheric lifetime of CO₂ of millennia to thousands of years (Archer and Brovkin, 2008).

Extensive $\delta^{13}\text{C}$ work has been completed for six sections in the Nanpanjiang Basin by Lehrmann et al. (2015) and the values from subsection 1 and 2 have been compared to data for these six sections along the extinction boundary. The values from both subsections of the Tianwan section determined in this study fit data from the additional six sections; an increase pre extinction and decrease post extinction in $\delta^{13}\text{C}$ values (Lehrmann et al., 2015). Further stable isotope data of $\delta^{13}\text{C}$ must be done for the Tianwan section in order to gain a more complete understanding; however, the analyses completed thus far add further evidence of paleoenvironmental conditions during the late Permian and early Triassic including that of increased CO₂ potentially resulting in ocean acidification; acidic conditions, however, cannot be entirely extrapolated from the $\delta^{13}\text{C}$ and $\delta^{18}\text{O}$ data collected herein. While not used in this

research study as monetary constraints did not allow for testing, $\delta^{11}\text{B}$ and $\delta^{44}\text{Ca}$ isotopes are incredibly useful tools for understanding the mechanisms of the late Permian mass extinction and are discussed in the Future Work section.

Diagenetic Structures: Stylolites are secondary aspects of this study as they do not have a quantitative component to their analysis but rather a qualitative interpretation based on their stratigraphic location. In general, they occur most around the extinction boundary, and more specifically the truncation surface as detailed by Lehrmann et al. (2015) (Figures 17 and 18). Stylolites are defined as irregular lines in vertical cut sections of carbonate rocks as a result of pressure dissolution that can result in centimeters of rock lost from the sedimentary record thereby obscuring paleoenvironmental data (Kershaw et al., 2012). This research posits the opposite—that stylolites, if caused by chemical and not just pressure dissolution, document oceanic and chemical conditions at the time and shortly after deposition. The issue with stylolites lies in the fact that their origin and extent are incredibly understudied. Rather for subsections 1 and 2, a synthesis of the position of stylolites with respect to the subsections can be made. In the Sichuan and Chongqing sites in the Nanpanjiang Basin, there has yet to be a transition that does not exhibit stylolites along the extinction boundary by recorded by any researcher (Kershaw et al., 2012). More field research is needed at additional Permian-Triassic boundaries to determine if the formation of stylolites is associated with dissolution by ocean acidification, which anecdotally seems plausible, but this fact alone seems far from coincidence, especially considering fossil data suggests ocean acidification occurred. Moreover, stylolites are understudied so gaining more information on their formation is critical to future studies. The Future Work section provides

a synthesis of stylolite growth and characterization which proves useful to the understanding of stylolite formation.

Aragonite fans at the Permian-Triassic boundary have been noted from personal communication with Lehrmann in the Tianwan section above the truncation surface and are detailed as extensive throughout the Nanpanjiang Basin (Payne and Kump, 2007).

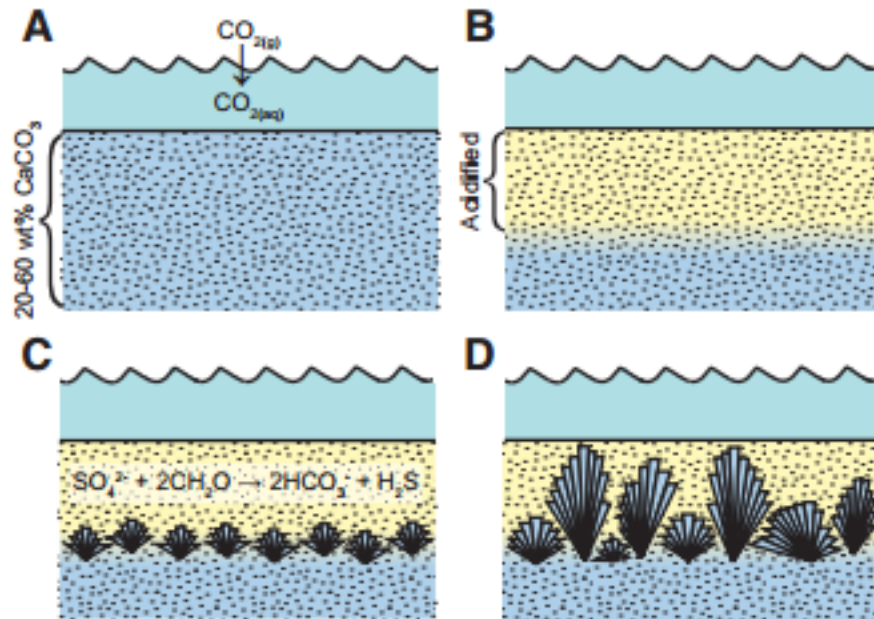


Figure 19. Proposed aragonite fan deposition model as a result of lowered pH proposed by Greene et al., 2012. (A) Demonstrates the assimilation of CO_2 into the oceans, (B) demonstrates the acidified sediment layer composed primarily of calcium carbonate due to CO_2 assimilation reducing the pH, (C) demonstrates sulfate reducing bacteria at the unacidified-acidified boundary increasing the pH to allow for aragonite fan deposition, and (D) demonstrates the extent of aragonite fan growth in the acidified layer of sediment.

Greene et al. (2012) take an alternative approach to the ocean acidification induced extinction event (Triassic-Jurassic) by analyzing diagenetically induced aragonite fans. Diagenetic structures have been largely ignored because they have been thought to be secondary and unimportant as they precipitate after deposition (Greene et al., 2012). However, the Black Bear Ridge units (British Columbia) display unique aragonite fans at the

boundary of the extinction event, leading the authors to believe the structures are uniquely tied to ocean acidification (Greene et al., 2012). By analyzing nucleation surfaces, growth patterns, and isotopic data, the authors were able to postulate that diagenetic structures are incredibly useful to the understanding of the origin of mass extinction events. Figure 14 shows the aragonite fan deposition model thought to be a result of ocean acidification through the acidification of calcium carbonate sediments as a result of increased $p\text{CO}_2$ and the presence of sulfate reducing bacteria at the unacidified-acidified boundary increasing the pH to allow precipitation of aragonite fans. Data from the Tianwan section, specifically location of aragonite fans (Figures 17 and 18) fits the model of aragonite fan deposition as their location is shortly after the mass extinction (within the early Triassic microbialites) in the presumably acidified sediments. Further research, specifically qualitative data collection, on aragonite fans in the Tianwan section must be completed; however, the presence of aragonite fans is yet another indicator of large-scale ocean acidification during the late Permian mass extinction.

FUTURE WORK

The methods discussed in this section would have proved useful to the understanding of paleoenvironmental conditions during the late Permian mass extinction primarily in respect to ocean acidification; but, monetary restrictions limited the study to that of faunal succession and traditional stable isotopes, both of which proved useful for the scope of this study. Each method is discussed in terms of their advantages and limitations

Stable Isotopes: In the case of ocean acidification, boron can be used as a paleo-pH indicator as $\delta^{10}\text{B}$ and $\delta^{11}\text{B}$ stable isotopes from foraminifera are a unique and understudied proxy for paleo-pH reconstructions. Two species of boron exist in seawater: $\text{B}(\text{OH})^3$ is more abundant at pHs below 7 and $\text{B}(\text{OH})^{4-}$ is more abundant at pHs above 11 (Maslin and Swann, 2006). Of particular interest to paleo-ocean acidification research are biogenic sources of calcium carbonate as they preferentially take up $\text{B}(\text{OH})^{4-}$ meaning $\delta^{11}\text{B}$ precipitated in calcite is used as a function of seawater pH (Maslin and Swann, 2006). Uniform shell size of the foraminifera is needed for isotope analysis as major shifts have been noted in previous experiments with varying shell size and partial dissolution of said shells (Maslin and Swann, 2006). This particular facet of using boron isotopes can be incredibly difficult to maintain as diagenetic processes and biological diversity all cause variation in shell size (Maslin and Swann, 2006). Furthermore, an understanding of pK^*B (boric acid) is needed to explain $\delta^{11}\text{B}$ as a function of pH which is then dependent on temperature, salinity, and pressure during the time of deposition. Oftentimes, these values are assumed by the researcher further adding to the uncertainty of using boron as a proxy of ocean acidification (Maslin and Swann, 2006). By understanding the strengths and weaknesses of the potential stable isotopes used as

proxies, particularly boron for ocean acidification, new insight can be added to the understanding of how and why the late Permian mass extinction occurred.

Griffith et al. detail the use of $\delta^{44}\text{Ca}$ as a tool to reconstruct paleoclimates and paleoceanographic conditions, specifically preserved in carbonate rocks. An issue that arises with the use of carbonate rocks is that they are susceptible to diagenetic processes through dissolution (Griffith et al., 2015). Of particular interest is widespread dissolution due to ocean acidification which is oftentimes marked by abrupt and immense carbon release into the ocean-atmosphere system (Griffith et al., 2015). Griffith et al.'s paper investigates carbonate dissolution as a result of ocean acidification during the Paleocene-Eocene Thermal Maximum and explains the large variation (0.8 parts per million) in $\delta^{44}\text{Ca}$ as a result of ocean acidification. Their results showed that one can compare $\delta^{44}\text{Ca}$ values to that of the global record and if they do not agree, it can be inferred that dissolution is responsible for the increase in variation (Griffith et al., 2015). By placing a quantitative value on ocean acidification proxies, one will be able to compare values of known diagenetic origin to those that require further evidence and analysis (Griffith et al. 2015). This article is imperative to understanding proxies of paleo pH as they add to the hypothesis that the late Permian mass extinction was a result of ocean acidification. With stable isotopes as a strong base of quantitative data, one is then able to analyze qualitative data such as diagenetic structures and processes.

Diagenetic Structures: Rolland et al. (2011) detail the theoretical growth of stylolites and the accompanying style of stress associated with each respective stylolite. They also compute the dissolution rate as it relates to stress. By outlining how stylolites are formed and the differences between the differing geometries, one will be better able to understand

the localized stress related to the style of stylolite and gain a broader sense of the structural evolution; whether it is chemically induced or of pure structural form is up for debate (Rolland et al., 2011).

Koehn et al. (2016) begin their paper by outlining what defines a stylolite and the conditions upon which they grow (intergranular pressure, diagenesis, and tectonic strain). By modeling layer-dominated stylolites, the authors were able to understand the structural evolution which then enabled them to classify the stylolites based on shape and suture structure into four unique categories (Koehn et al., 2016). For the scope of this thesis, one is able to gather that rectangular style type stylolites are what one should research further because they exemplify chemical compaction (Koehn et al., 2016). Because stylolites are only used when interpreting structural stress via pressure, their use in chemical dissolution has not been proposed. Their proposed use as indicators of chemical dissolution in this study has the potential to serve as parameters of oceanic conditions during and after deposition, but further research and modeling must be published in order to do so which is both an opportunity and drawback to focusing on ocean acidification as a kill mechanism during the late Permian mass extinction.

If one understands the origin and development of stylolites, one will then be able to apply this information to the study of stylolites as a result of chemical rather than pressure dissolution, further providing insight into boundaries of ocean acidification. While factual knowledge is gained through understanding the modeling of stylolites due to tectonic stress, the formation of stylolites semi-penecontemporaneously in respect to sub-marine and shallow marine environments must be investigated. So far, there is little research on either aspect

adding to the overall need for investigation on the use of stylolites as proxies of ocean acidification.

\

CONCLUSION AND IMPLICATIONS

As an overview, faunal succession data from subsections 1 and 2 suggests a general decrease in diversity (Figures 9 and 12) and increase in taxa specific dominance (Figures 8 and 11). Moreover, the R-squared values for both Simpson's and Simpson's Index of Diversity are believed to be unimportant aspects to the general understanding of the kill mechanisms as it is important to note the erratic nature of the graphs in Figures 8 and 11. The erratic nature points to the irregularity of marine conditions and the response of marine organisms during the late Permian and early Triassic. This data matches what would be expected from a mass extinction event; a decrease in diversity and an increase in taxa specific dominance, or "disaster taxa" coupled with erratic changes in the environment during and post extinction (Correa and Baker, 2011). Hypercalcifiers suffered the most in terms of decreased abundance; gastropods (moderate calcifiers) then filled the niche of hypercalcifiers due to their ability to buffer fluids that govern calcium carbonate precipitation likely affected by ocean acidification conditions (Knoll et al., 2007).

In terms of stable isotope geochemistry analysis, $\delta^{13}\text{C}$ and $\delta^{18}\text{O}$ were used to determine paleoenvironmental conditions that would shed light on potential kill mechanisms of the late Permian mass extinction, specifically ocean acidification. $\delta^{13}\text{C}$ excursion values for subsections 1 and 2 revealed an increase in CO_2 levels pre and during mass extinction. After the mass extinction, CO_2 levels decreased (Figures 13 and 15). While exact atmospheric CO_2 concentrations are not quantified using the $\delta^{13}\text{C}$ excursion values, they do reveal the general increase in CO_2 before and during extinction followed by a general decrease that would accompany the emplacement of a large igneous province, in this case the Siberian Traps (Bond and Grasby, 2016). $\delta^{18}\text{O}$ excursion values for both subsection 1 and 2

revealed a general decrease in global average temperature before and during mass extinction then a general increase in levels post mass extinction. The general decrease then increase in global average temperature fits what is to be expected as a result of the Siberian Traps emplacement (Bond and Grasby, 2016). Both the faunal succession and stable isotope geochemistry values match that of published data further adding to the overall understanding of the mechanisms of the late Permian mass extinction.

While a secondary component to this thesis, the analysis of stylolites and aragonite fans provided potential as well as additional proxies of ocean acidification respectively. The location of stylolites was documented in a general fashion around the truncation surface that coincides with the mass extinction boundary (Figure 17). This observation could indicate that stylolites potentially form as a result of chemical rather than pressure dissolution as documented in literature, but this is a hypothesis that deserves more research (Kershaw et al., 2012). Chemical dissolution driven formation of stylolites was based loosely upon the aragonite fan deposition model presented by Greene et al. (2012) that explains the acidification of calcium carbonate sediment as a result of ocean acidification and interplay of sulfate reducing bacteria which allow aragonite fans to nucleate at the unacidified-acidified boundary (Figure 19). Aragonite fans have been documented in subsections 1 and 2 directly after the extinction in the microbial boundstone unit as well as at additional Permian-Triassic boundary localities in the Nanpanjiang Basin (Lehrmann, personal communication). Because aragonite fans are hypothesized to be a result of ocean acidification, their presence directly above the late Permian mass extinction boundary is an additional indicator that ocean acidification is a likely kill mechanism that occurred as a result of the Siberian Traps emplacement. Limitations of this thesis lie in the fact that no deep marine rock record is

available for either subsection so kill mechanisms such as seafloor anoxia cannot be analyzed. Moreover, fossils inherently are an imperfect record of environmental conditions because they do not represent the entirety of any system (Kershaw et al., 2012). However, their presence, while not complete, is the only indicator of biotic diversity during the late Permian mass extinction.

The late Permian mass extinction is a complex 252 million year old mystery. Its clues as to the demise of 90% of marine and 70% of terrestrial organisms are gradually becoming unveiled as technology and interest progresses. Perhaps the most interesting facet of the late Permian mass extinction is its applications to modern oceanic conditions and trends. Recent estimates for the total CO₂ release during the P-T over 400 kyr was ~0.1 to 1.0 PgC whereas 2008 was 9.9 PgC (Bond and Grasby, 2016). While the percentage of species extinction during the late Permian is startling, current extinction rates are ten to one-hundred times greater than any previous mass extinction (Turley and Gattuso, 2012). This has led to the general consensus that Earth is in the midst of a sixth mass extinction as a result of anthropogenic induced climate change (Zalasiewicz et al., 2010). The current pH of the ocean is 8.1 but projected pH is expected to reach 7.7 to 7.9 by 2100 and the effects are not only biological but social and economic as well (Turley and Gattuso, 2012).

While the Law of Uniformitarianism states the present is key to understanding the past, evidence of past climate change events could provide answers to current climate change driven environmental issues, specifically that of ocean acidification, as a result of increased anthropogenic CO₂. It would appear that CO₂ dissolving into Earth's oceans could serve as a remedial exchange to end rising, global temperatures, but it has devastating, long-term consequences. As CO₂ dissolves into the ocean, it reacts with water to form carbonic acid

which then reduces the pH of the ocean. This lowered pH has been documented to harm shell building marine organisms through dissolution of their carbonate shells (The Ocean Portal Team, 2016). Additional physiological processes affected by lowered pH include ion transport, enzyme activity, and protein function (Turley and Gattuso, 2012). These effects are oftentimes taxa specific with hypercalcifiers most heavily affected, which is a trend witnessed by Permian-Triassic organisms in Figures 7 and 10 (Wittmann and Pörtner, 2013). The main focus of ocean acidification research has centered on the biologic response to lowered pH on various marine organisms, primarily corals, planktons, echinoderms, mollusks, crustaceans, and fish (Brander et al., n.d.). Fish, coral, and plankton are the most sensitive to ocean acidification and have the potential to alter the biologic composition of the oceans as well as society's dependence on the ocean for various uses (Brander et al., n.d.) Moreover, the base of marine food chains (~50%) is primarily composed of planktons adding to the synergistic and detrimental effects on all biologic levels of ocean acidification (Wittman and Pörtner, 2013).

The social and economic implications of anthropogenic induced ocean acidification are far-reaching and vast, but in totality are incredibly understudied. This is largely due to the fact that global population, supply, demand, and oceanic services are always changing (Brander et al., n.d.). Economically, ~80% of world trade takes place across the ocean making it an artery of growth and development (Turley and Gattuso, 2012). Moreover, oceanic resources such as aquaculture and tourism provide work for over 38 million people, 95% of which live in developing countries (Turley and Gattuso, 2012). As a result of ocean acidification, it is projected that \$870 billion will be lost from recreational economic services provided by the ocean in 2100, and even more unfortunate, this projection does not account

for coastal protection by reefs and loss of biodiversity. Loss of diversity can be quantified by inflation of marine food prices but it is difficult to project those values. By the year 2050, catch potentials are estimated to decline by 20 to 30% globally and have the potential to decrease more if biodiversity loss increases as well (Brander et al., n.d.).

Socially, it is important to understand that vulnerability with respect to ocean acidification is spatial; coastal communities and those that rely on services provided by the ocean are most susceptible and, therefore, have a low capacity to adapt to changing environmental conditions (Brander et al., n.d.). As stated previously, a large number of people are dependent on the ocean for their livelihood, but more innately they are also dependent on the ocean as their source of food (Turley and Gattuso, 2012). In the United States, 16% of protein is provided through marine organisms and is the main source of protein for over 1 billion people (Turley and Gattuso, 2012). Ocean acidification has the potential to create food security issues across the globe and it can even be argued that the preservation of the services provided by the ocean is a human right. This creates the need for international policy action because while the literature surrounding social and economic implications of ocean acidification is sparse, what is published is riveting and cause for global concern.

In order to create efficient and encompassing international policy, the mechanisms and effects of ocean acidification must be understood. Considering this understanding is not yet complete, it begs the question of when is too late to institute international policy? Is it already too late? Ocean acidification was first recognized by the Intergovernmental Panel on Climate Change only ten years ago making its presence as an international concern current and pressing (Turley and Gattuso, 2012). In terms of policy facilitation, the United Nations

serves as the most effective platform to execute action but local jurisdiction can take place through amending various acts, introducing laws and policies, and increasing awareness of the effects of ocean acidification through educational programs and seminars. While research is in development, there is nothing barring citizens from understanding the implications of their actions. The underlying cause of ocean acidification is climate change and the effects of climate change are well understood (Zalasiewicz et al., 2010). In order to mitigate the effects of ocean acidification, one must mitigate the effects of climate change. Commonly cited methods such as reducing a given individual's carbon footprint, introducing renewable forms of energy, buying local goods, and simply educating oneself on what it means to be a mindful inhabitant of Earth will enable a more complete awareness of one's actions and their effect on valuable environmental resources.

LITERATURE CITED

- Archer, David and Victor Brovkin, 2008. The millennial atmospheric lifetime of anthropogenic CO₂. *Climatic Change*, 90: 283-297.
- Bond, David P.G. and Stephen E. Grasby, 2016. On the causes of mass extinctions. *Palaeogeography, Palaeoclimatology, Palaeoecology*, 1-27.
- Bottjer, David J., Matthew E. Clapham, Margaret L. Fraiser, and Catherine M. Powers, 2008. Understanding mechanisms for the end-Permian mass extinction and the protracted Early Triassic aftermath and recovery. *GSA Today*, 1-10.
- Brander, Luke M., Daiju Narita, Katrin Rehdanz, and Richard S.J. Tol, n.d. The economic impacts of ocean acidification. Thesis, Institute for Environmental Studies, VU University, Amsterdam, the Netherlands.
- Capdevielle, Jillian, n.d. Neritid gastropods adapted to different pH environments: spatial, temporal, and abiotic factors affecting life history traits of marine and freshwater snails. Thesis, Environmental Science Policy and Management, University of California, Berkeley.
- Chen, Jun, Tyler W. Beatty, Charles M. Henderson, and Harry Rowe, 2009. Conodont biostratigraphy across the Permian-Triassic boundary at the Dawen section, Great Bank of Guizhou, Guizhou Province, South China: implications for the late Permian extinction and correlation with Meishan. *Journal of Asian Earth Sciences*, 36: 442-458.
- Correa, Adrienne M.S. and Andrew C. Baker, 2011. Disaster taxa in microbially mediated metazoans: how endosymbionts and environmental catastrophes influence the adaptive capacity of reef corals. *Global Change Biology*, 17 (1): 68-75.

- DiMichele, W.A., Stein, W.E., Bateman, R.M., 2001. Ecological sorting of vascular plantclasses during the Paleozoic evolutionary radiation. In: Allmon, W.D., Bottjer, D.J. (Eds.), *Evolutionary Paleocology*. Columbia University Press, New York, 285-335.
- Droser, Mary L., David J. Bottjer, Peter M. Sheehan, George R. McGhee Jr., 2000. Decoupling taxonomic and ecologic severity pf Phanerozoic marine mass extinctions. *Geology*, 28 (8): 675-678.
- Erwin, Douglas H., 1994. The Permo-Triassic extinction. *Nature*, 367: 231-236.
- Greene, Sarah E., David J. Bottjer, Frank A. Corsetti, William M. Berelson, and John-Paul Zonneveld, 2012. A subseafloor carbonate factory across the Triassic-Jurassic transition. *GEOLOGY*, 40 (11): 1043-1046.
- Griffith, Elizabeth M., Matthew S. Fantle, Anton Eisenhauer, Adina Paytan, and Thomas D. Bullen, 2015. Effects of ocean acidification on the marine calcium isotope record at the Paleocene-Eocene Thermal Maximum. *Earth and Planetary Science Letters*, 419: 81-92.
- Gorelick, Root, 2006. Combining richness and abundance into a single diversity index using matrix analogues of Shannon's and Simpson's Indices. *Ecography*, 29 (4): 525-530.
- Heltshe, James F., and Nancy E. Forrester, 1985. Statistical evaluation of the Jackknife estimate of diversity when using quadrat samples. *Ecology*, 66 (1): 107-111.
- Hönisch, Barbel, Andy Ridgwell, Daniela N. Schmidt, Ellen Thomas, Samantha J. Gibbs, Appy Sluijs, Richard Zeebe, Lee Kump, Rowan C. Martindale, Sarah E. Greene, Wolfgang Kiessling, Justin Ries, James C. Zachos, Dana L. Royer, Stephen Barker, Thomas M. Marchitto Jr., Ryan Moyer, Carlos Pelejero, Patrizia Ziveri, Gavin L.

- Foster, and Branwen Williams, 2012. The Geological Record of Ocean Acidification. SCIENCE, 335: 1058-1063.
- Ikanov, Alexei V., He Huayiu, Yan Liekun, Ryabov, Viktor V. Shevko Artem Y. Paleskii Stanislav V., Nikolaeva, Irina V., 2013. Siberian Traps large igneous province: Evidence for two flood basalt pulses around the Permo-Triassic boundary and in the Middle Triassic, and contemporaneous granitic magmatism. Earth Science Reviews, 122: 58-76.
- International Atomic Energy Agency. “Stable Isotopes.” 2017.
<https://www.iaea.org/topics/isotopes/stable-isotopes>.
- Jin, Y.G., Y. Wang, W. Wang, Q.H. Shang, C.Q. Cao, and D.H. Erwin, 2000. Pattern of marine mass extinction near the Permian-Triassic boundary in South China. Science, 289 (5478): 432-436.
- Kershaw, Stephen, Sylvie Crasquin, Yue Li, Pierre-Yves Collin, and Marie-Béatrice Forel, 2012. Ocean Acidification and the End-Permian Mass Extinction: To What Extent does Evidence Support Hypothesis?. Geosciences, 2: 221-234.
- Knoll, Andrew H., Richard K. Bambach, Jonathon L. Payne, Sara Pruss, and Woodward W. Fischer, 2007. Paleophysiology and end-Permian mass extinction. Earth and Planetary Science Letters, 256: 295-313.
- Knoll, Andrew H. and Woodward W. Fischer, 2011. Skeletons and ocean chemistry: the long view. Ocean Acidification, 4: 67-82
- Koehn, D., M.P. Rood, N. Beaudoin, P. Chung, P.D. Bons, and E. Gomez-Rivas, 2016. A new stylolite classification scheme to estimate compaction and local permeability variations. Sedimentary Geology, 346: 60-71.

- Lehrmann, Daniel J., John M. Bentz, Tanner Wood, Alexa Goers, Ryan Dhillon, Sara Akin, Xiaowei Li, Jonathon L. Payne, Brian M. Kelley, Katja M. Meyer, Ellen K. Schaal, Marina B. Suarez, Meiyu Yu, Yanjiao Qin, Rongxi Li, Marcello Minzoni, and Charles M. Henderson, 2015. Environmental controls on the genesis of marine microbialites and dissolution surface associated with the end-Permian mass extinction: new sections and observations from the Nanpanjiang Basin, South China. *Palaaios*, 30: 529-552.
- Lehrmann, Daniel J., Jiayong Wei, and Paul Enos, 1998. Controls on facies architecture of a large Triassic carbonate platform: the Great Bank of Guizhou, Nanpanjiang Basin, South China. *Society for Sedimentary Geology*, 68 (2): 311-326.
- Levin, Lisa A. and Nadine Le Bris, 2015. The deep ocean under climate change. *Science*, 350 (6262): 766-768.
- Maslin, M.A., and G.E. Swann, 2006. Isotopes in Marine Sediments. In: Leng, 2006, *Isotopes in Paleoenvironmental Research. Developments in Paleoenvironmental Research*. Springer, The Netherlands. 10: 227-272.
- National Science Foundation. "Global Extinction: Gradual Doom as Bad as Abrupt." Spaceref. 2012. <http://www.spaceref.com/news/viewpr.html?pid=35965>
- The Ocean Portal Team. "Ocean Acidification." Ocean Portal. Smithsonian National Museum of Natural History, 2016. <http://ocean.si.edu/ocean-acidification>
- Ogden, Darcy E. and Norman H. Sleep, 2011. Explosive eruption of coal and basalt and the end-Permian mass extinction. *Current Issue*, 109 (1): 59-62.
- Payne, Jonathan L., Daniel J. Lehrmann, David Follett, Margeret Seibel, Lee R. Kump, Anthony Riccardi, Demir Altiner, Hiroyoshi Sano, and Jiayong Wei, 2007. Erosional

- truncation of uppermost Permian shallow-marine carbonates and implications for Permian-Triassic boundary events. *Geological Society of America Bulletin*, 119 (7/8): 771-784.
- Payne, Jonathon L. and Lee R. Kump, 2007. Evidence for recurrent Early Triassic massive volcanisms from quantitative interpretation of carbon isotope fluctuations. *Earth and Planetary Science Letters*, 256: 264-277
- Petsios, Elizabeth and David J. Bottjer, 2016. Quantitative analysis of the ecological dominance of benthic disaster taxa in the aftermath of the end-Permian mass extinction. *Paleobiology*, 42 (3): 380-393.
- Rego, Brianna L., Steve C. Wing, Demir Altiner, and Jonathon L. Payne, 2012. Within- and among-genus components of size evolution during mass extinction, recovery, and background intervals: a case study of Late Permian through Late Triassic foraminifera. *Paleobiology*, 38 (4): 627-643.
- Rohde, Robert. 2009. CO₂ levels last 500 million years. AGU Blogosphere. “New Clue to Past CO₂ levels??” <http://blogs.agu.org/wildwildscience/2009/07/07/new-clue-to-past-co2-levels>.
- Rolland, Alexandra, Renaud Toussaint, Patrick Baud, Jean Schmittbuhl, Nathalie Conil, Daniel Koehn, Francois Renard, and Jean-Pierre Gratier, 2012. Modeling the growth of stylolites in sedimentary rocks. *Journal of Geophysical Research*, 117: 1-18.
- Shannon, C.E, 1948, A mathematical theory of communication. *The Bell System Technical Journal*, 27: 379-423, 623-656.
- Simpson, E.H., 1949. Measurement of Diversity. *Nature*, 163: 688.

- Turley, Carol and Jean-Pierre Gattuso, 2012. Future biological and ecosystem impacts of ocean acidification and their socioeconomic-policy implications. *Current Opinion in Environmental Sustainability*, 4 (3): 278-286.
- Twitchett, R.J., L. Krystyn, A. Baud, J.R. Wheeley, and S. Richoz, 2004. Rapid marine recovery after the end-Permian mass extinction event in the absence of marine anoxia. *Geology*, 32: 805-808.
- Whittaker, R.H., 1965. Dominance and diversity in land plant communities. *Science*, 144: 250-260.
- Wittmann, Astrid and Hans-O Pörtner, 2013. Sensitivities of extant animal taxa to ocean acidification. *Nature Climate Change*, 3: 995-1001.
- Zalasiewicz, Jan, Mark Williams, Will Steffen, and Paul Crutzen, 2010. The new world of the Anthropocene. *Environmental Science and Technology*. 44 (7): 2228-2231.

BIOGRAPHY

Maigan Dunlap was born in Lakenheath, England and lived most of her childhood in San Angelo, Texas. She graduated top 10% of her class from San Angelo Central High School and chose to attend Angelo State University to study geology Fall of 2013. While at Angelo State University, she was a student in the Honors Program where she became involved in various opportunities the program offered. Her sophomore year, she began research in the geosciences and was able to attend the Lehigh summer field camp her junior year. Both experiences allowed her to establish her love of field work and research within the realm of sedimentology.

After earning her Bachelors of Science in geology from Angelo State, Maigan will pursue a graduate degree in either paleoecology or carbonate biogeochemistry where she will investigate past environmental disasters and extinctions. Maigan plans to earn her doctorate and become a professor.